BSM heavy flavours, nonlocality, & searches in colliders

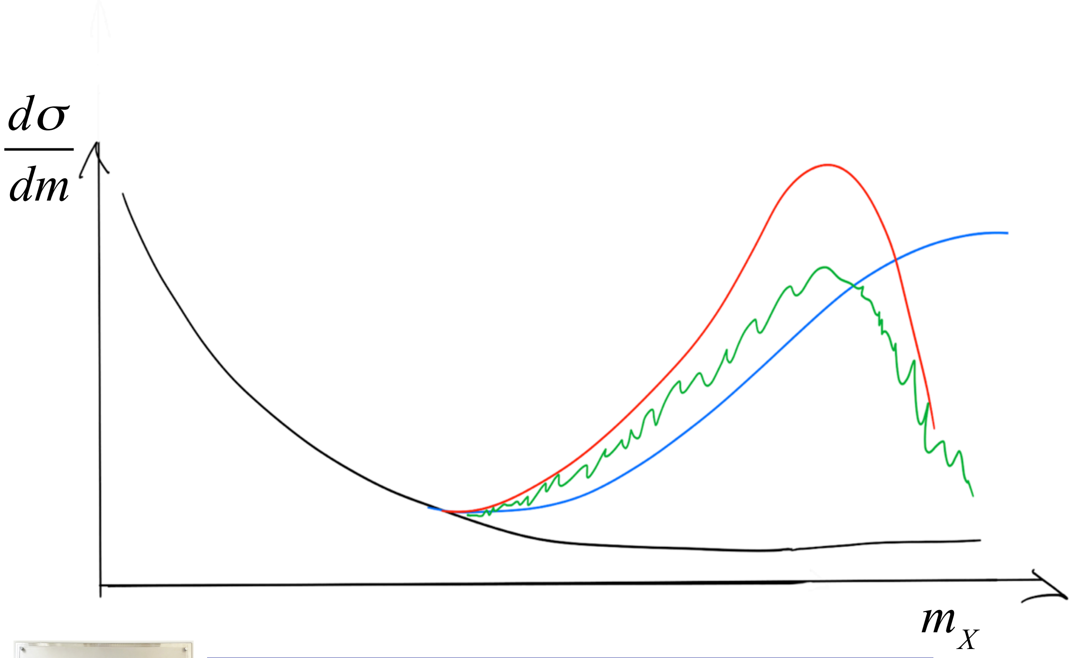

Taiwan Detector & Instr. Consortium

Introduction

- LHC experiments keep taking world's Highest Energy data: run 3
- Taiwan is building a new state-of-the-art HGCAL calorimeter for HLLHC. A huge project TW Chairs.
- Experimentalists & Theorists analyze and interpret new and old data.
- Focus of this talk is on BSM Heavy Particles, narrow or broad or towers.
- Can we constrain spectral densities from LHC data?

TW HEP has teamed up on building detectors for colliders to face the challenge!

10+2 years Higgs

LHC Run 3 ongoing: we are 12 years after the Higgs

CERN 10 years HIGGS boson discovery

Run-2 data are still being analyzed but a number of flagship analyses have been completed.

All measurements suggest what we have found is the SM Higgs.

- What makes the Higgs?
- What stabilizes the Higgs mass?
- Where is the New Physics?

Run 2: some excesses observed.
Run 3: improved searches, more parameter space covered.
HL-LHC: "Higgs precision"
improve our detectors, exploit the HL

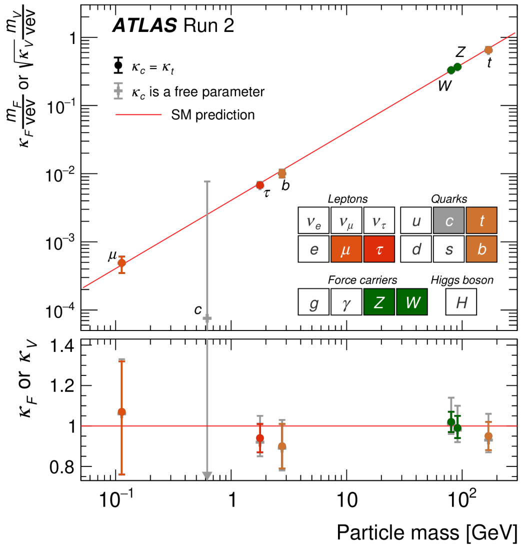

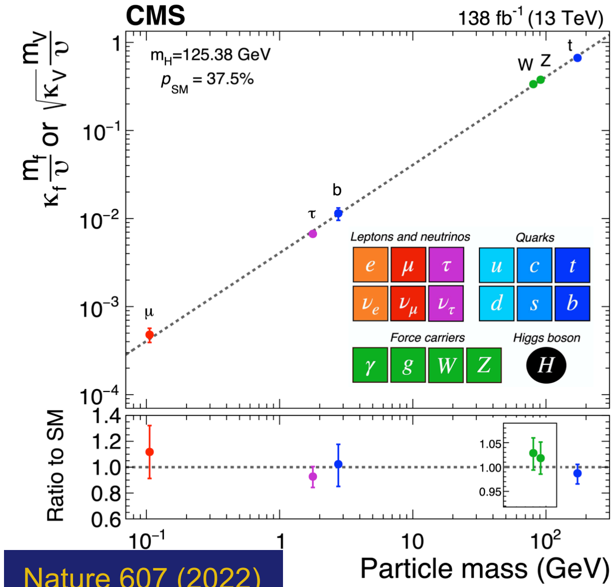

Nature 607 (2022)

LHC long-term plan

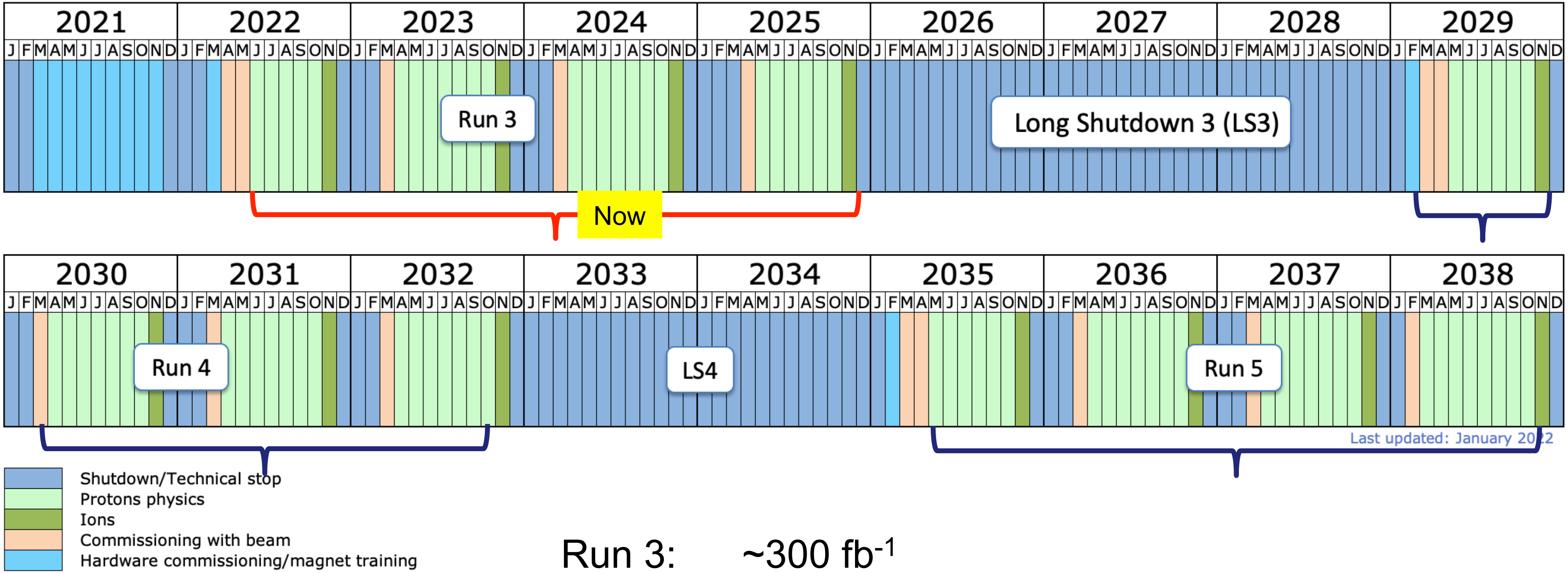

Run 3: ~300 fb^{-1}

HL-LHC: ~3000 fb^{-1}

BSM Flavours: new measurements

- (Heavy) Diphoton resonances and continuum:
  - ADD graviton continuum.
  - Spin-2 gravitons from bulk Randall-Sundrum model.
  - 2HDM scalar resonances.
  - Clockwork model resonance tower.

Spin-2 RS Graviton (warped ED)

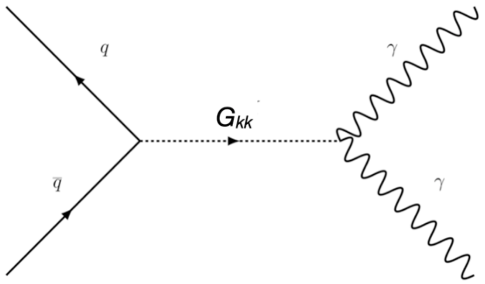

- X→HH, enhanced double-Higgs production:
  - Radion.
  - Spin-2 gravitons from bulk Randall-Sundrum model.
  - 2HDM CP-even scalar resonances.

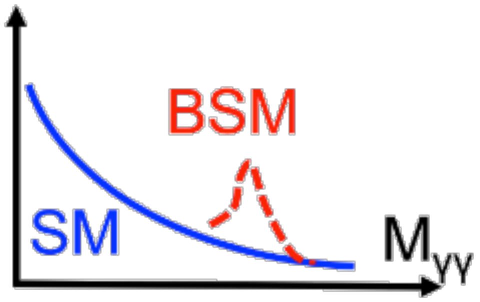

- VBF xsections including HH production:
  - Higgs-Higgs field scattering.
  - Using data constrain spectral densities of BSM operators?

Focus in diboson final states

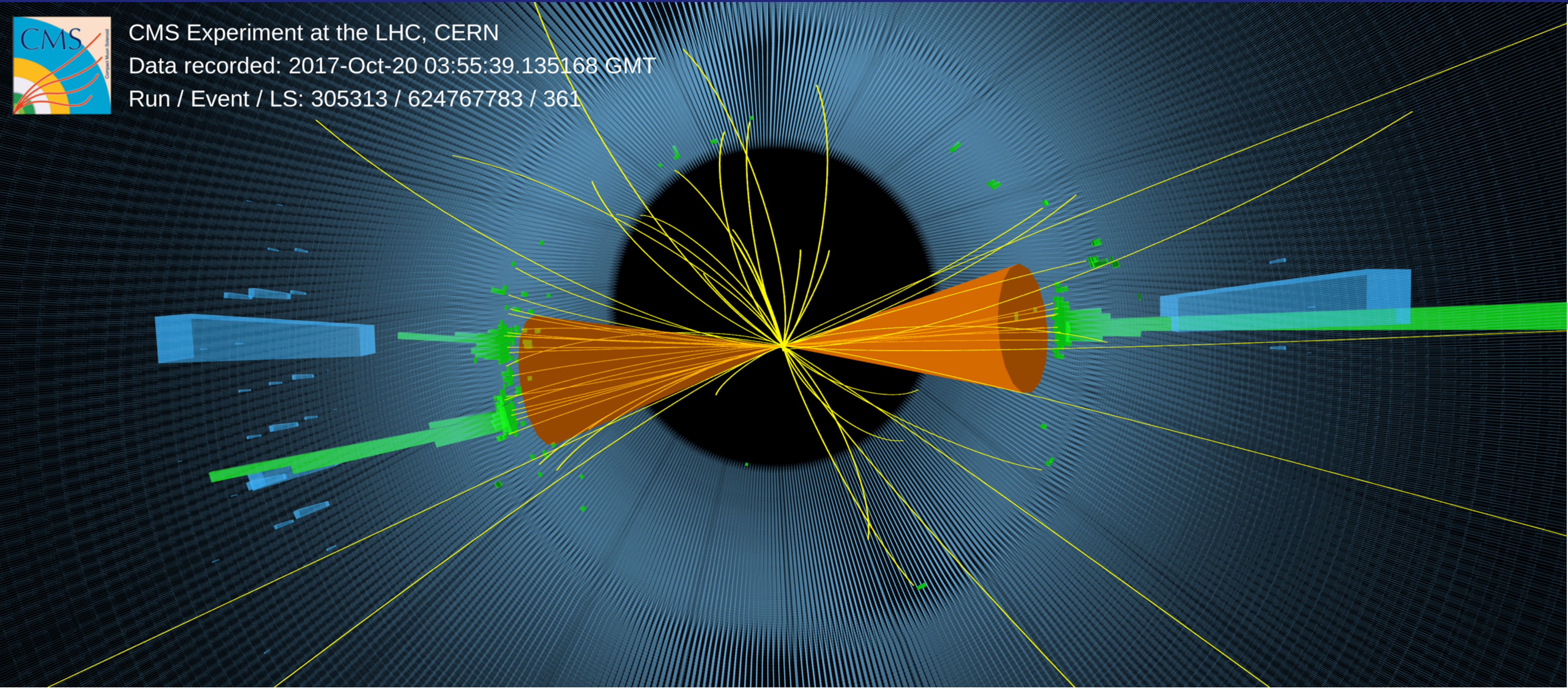

CMS diphoton search at ~m_Z

Submitted to PLB (28-May-2024)

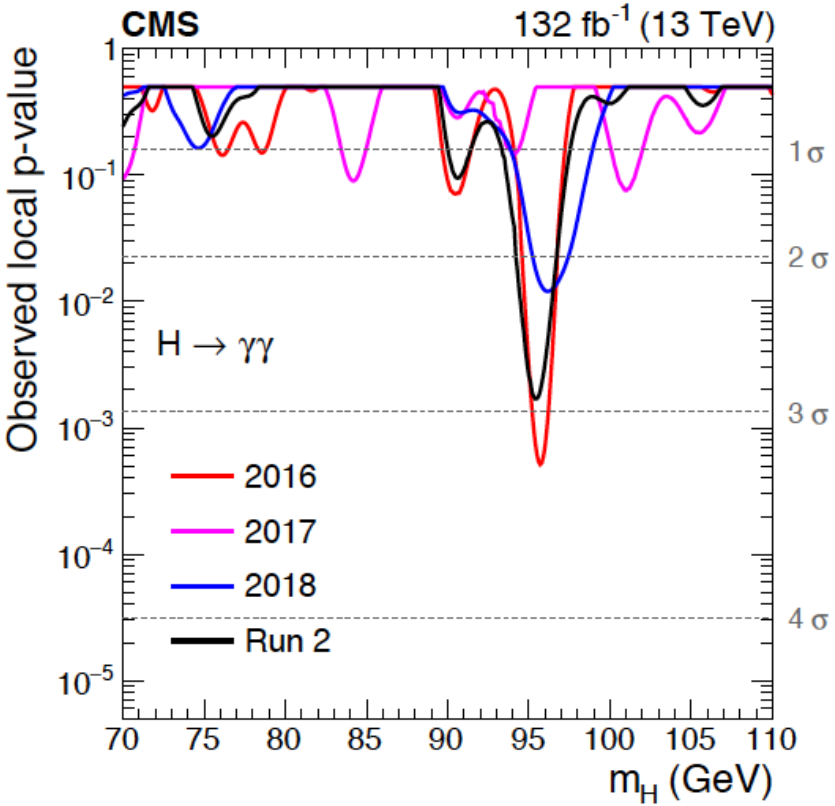

ATLAS diphoton search

Phys.Lett.B 822 (2021) 136651

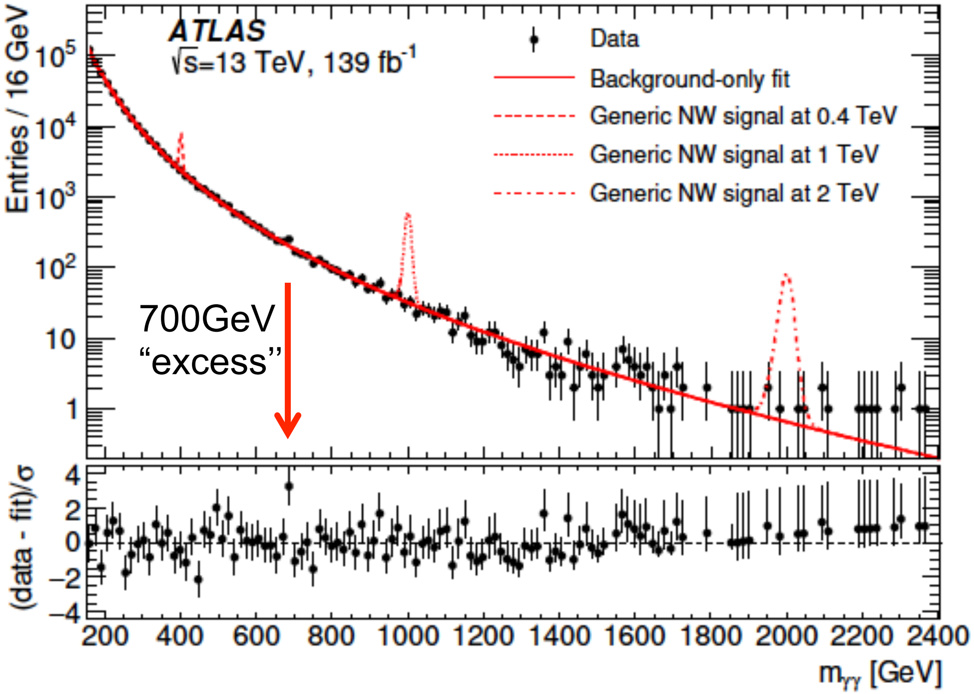

New: heavy diphoton search

arXiv:2405.09320 (15 May 2024)

Hsin-Yeh Wu PhD

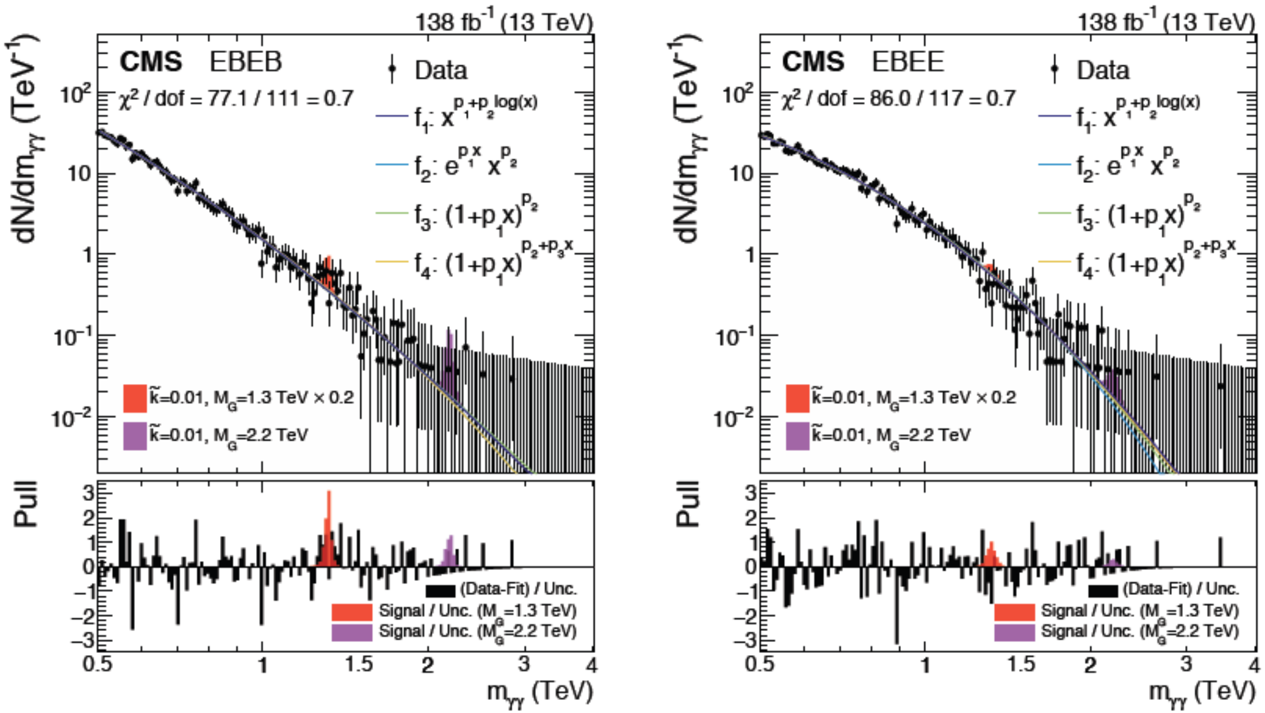

No obvious excesses in run 2.

We are working on a dedicated search for intermediated masses in run 2.

Heavy diphoton resonances

arXiv:2405.09320 (15 May 2024)

Hsin-Yeh Wu PhD

RS-graviton

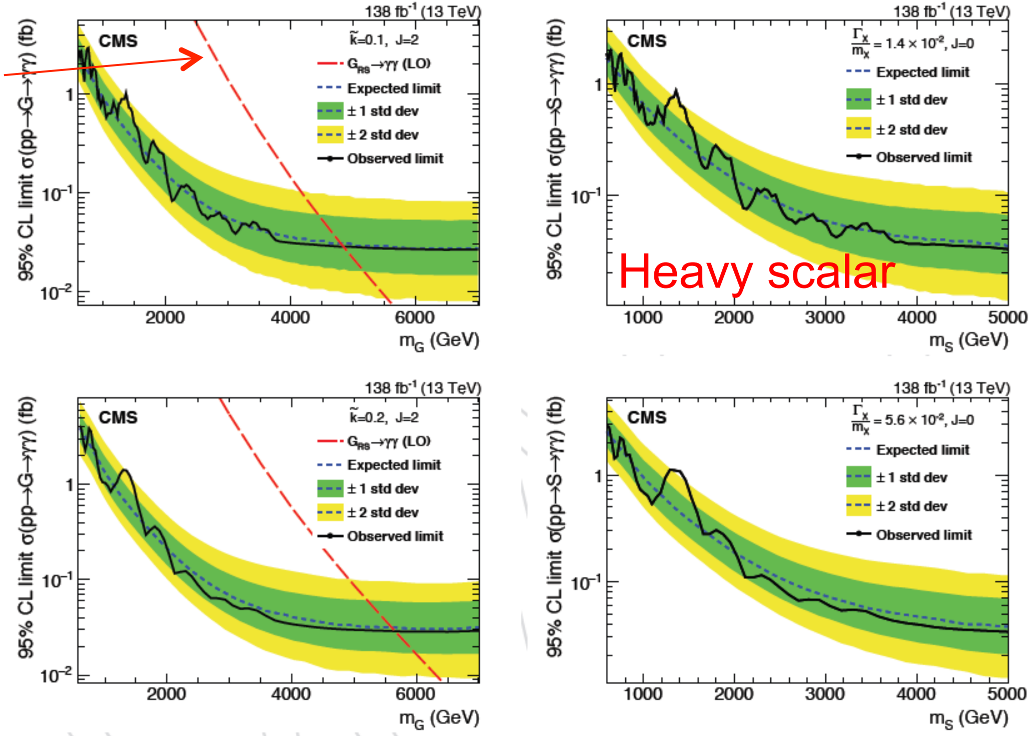

Figure 3: Expected and observed 95% CL upper limits on the product of the production cross section and branching fraction as a function of the RS graviton mass m_G (left) and heavy Higgs boson mass m_S (right) for the full Run 2 data set. The dotted red line is the LO theoretical cross section for the RS graviton. The rows correspond to different resonance widths. Expected 1 and 2 std. dev. limit bands are shown in green and yellow, respectively.

Largest excess at ~1.3TeV

Anomalous HH→bbWW production

arXiv:2403.09430 (March 2024)

SM production

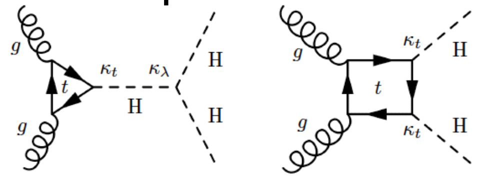

Figure 1: Leading-order Feynman diagrams of nonresonant Higgs boson pair production via gluon fusion in the standard model.

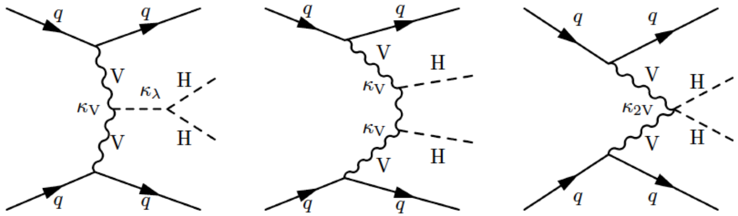

Figure 2: Leading-order Feynman diagrams of Higgs boson pair nonresonant production via vector boson fusion in the standard model.

Anomalous production

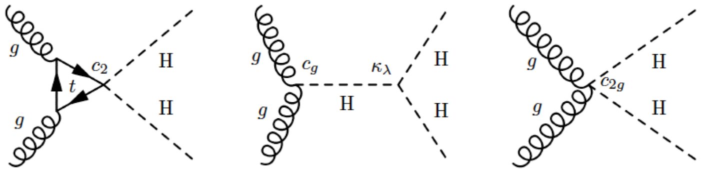

Figure 3: Leading-order Feynman diagrams of nonresonant Higgs boson pair production via gluon fusion with anomalous Higgs boson couplings.

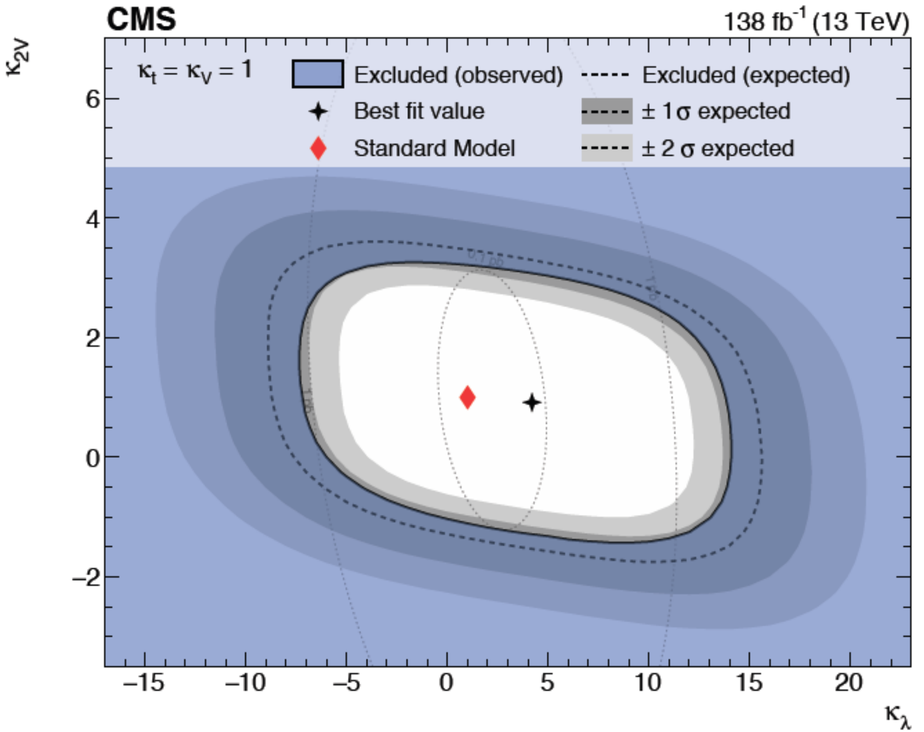

HVT: BSM spin-1 resonances

Coupling of resonance to SM fermions through mixing with the Eweak bosons.

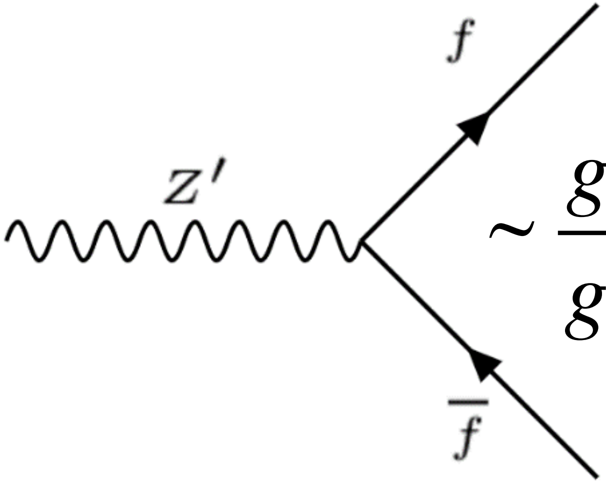

$$\sim \frac{g^2}{g_V} c_F$$

23. D. Pappadopoulo, A. Thamm, R. Torre and A. Wulzer, Heavy Vector Triplets: Bridging Theory and Data, JHEP 09 (2014) 060.

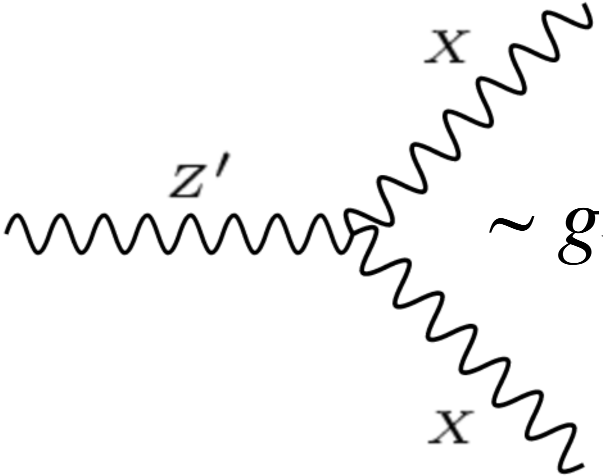

$$\sim g_V c_H$$

Heavy flavour triplet: W′, Z′

arXiv:2403.16926 (March 2024)

W′

Z′

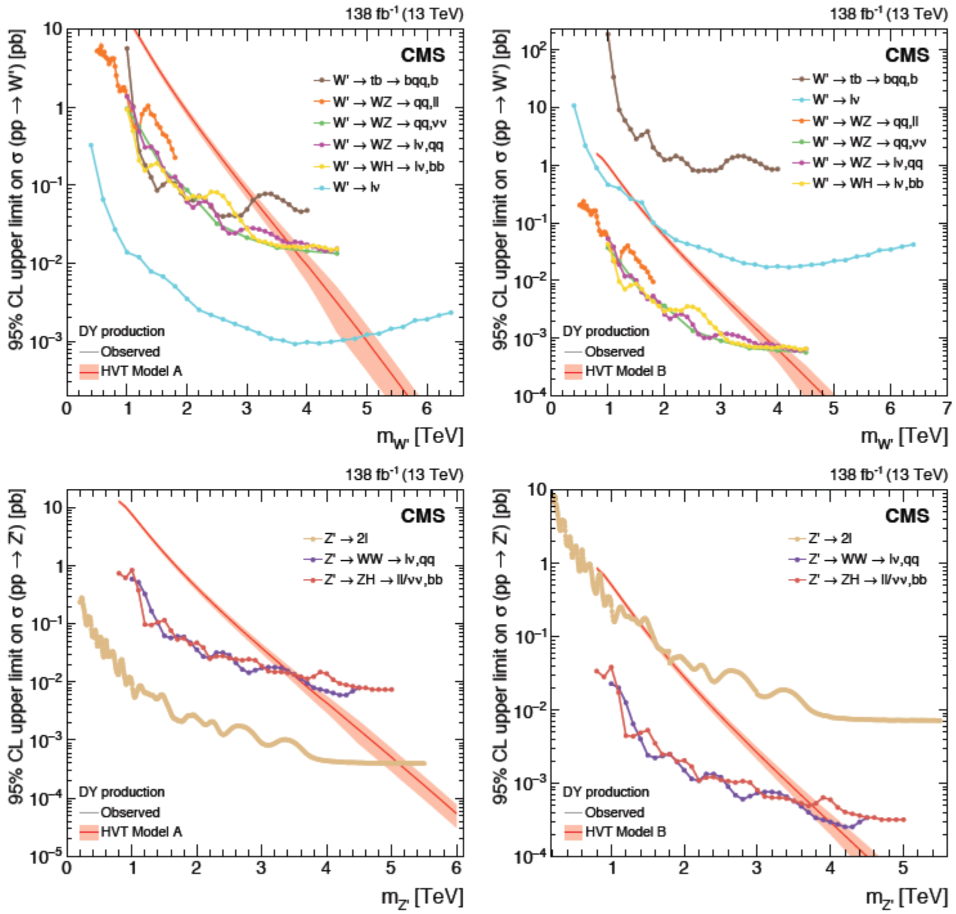

Heavy flavour triplet: W′, Z′

arXiv:2403.16926 (March 2024)

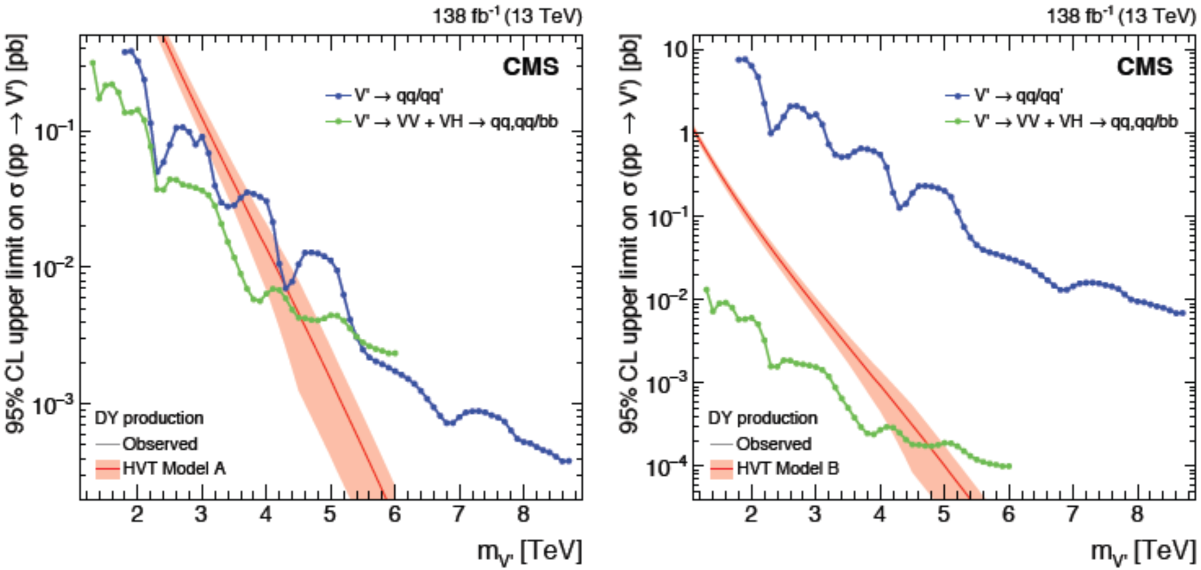

Figure 37: Observed upper limits, at 95% CL, on the Drell–Yan production cross section of (upper) W′, (middle) Z′, and (lower) combined V′ spin-1 resonances assuming branching fractions of the heavy vector triplet models (left) A and (right) B. The theory predictions from these models are also shown. Results from the VH [109–111] and VV channels [109, 111, 196, 197], as well as results from dijet [201], tb [199], $\ell\ell$ [198], and $\ell\nu$ [200] final states are also shown, for comparison.

Scalar→HH & Tensor→HH

arXiv:2403.16926
(March 2024)

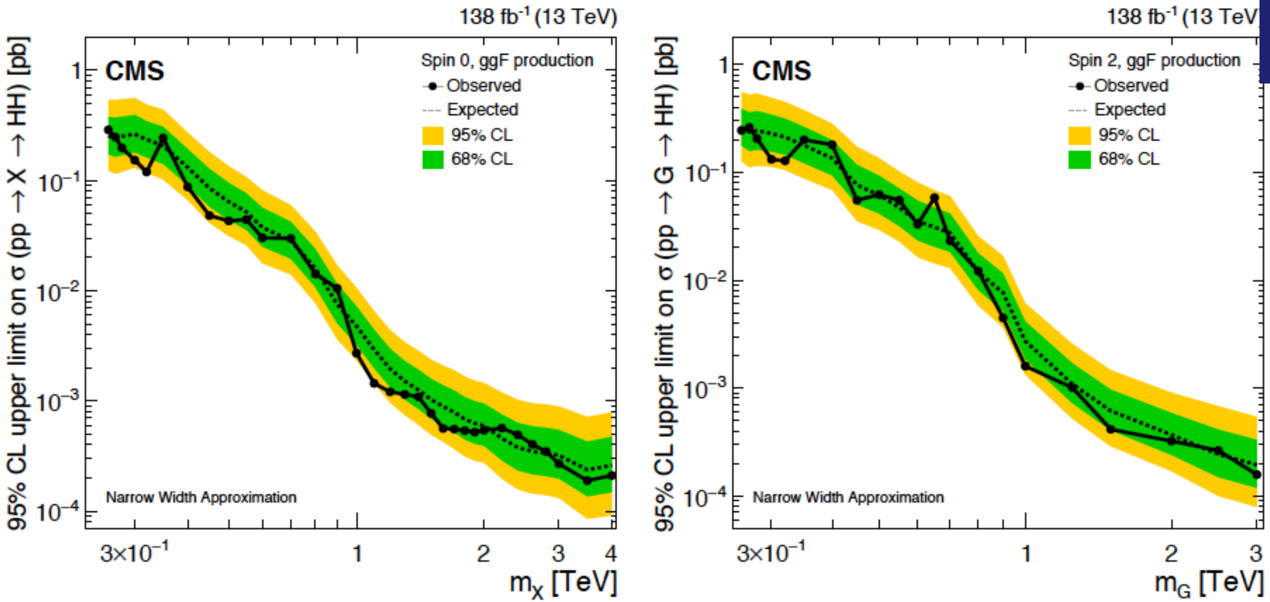

Figure 28: Search for $X \to HH/G \to HH$: Observed and expected 95% CL upper limits on the product of the cross section σ for the production of a (left) spin-0 resonance X and (right) a spin-2 resonance G, via gluon-gluon fusion, and the branching fraction $\mathcal{B}$ for the corresponding HH decay, as obtained from the combined likelihood analysis of all contributing individual analyses presented in this report and shown in Fig. 27. In addition to the limit from the combined likelihood analysis the 68 and 95% central intervals for the expected upper limits in the absence of a signal are shown as coloured bands.

Non-resonant HH→bbττ

arXiv:2404.12660
19-April-2024

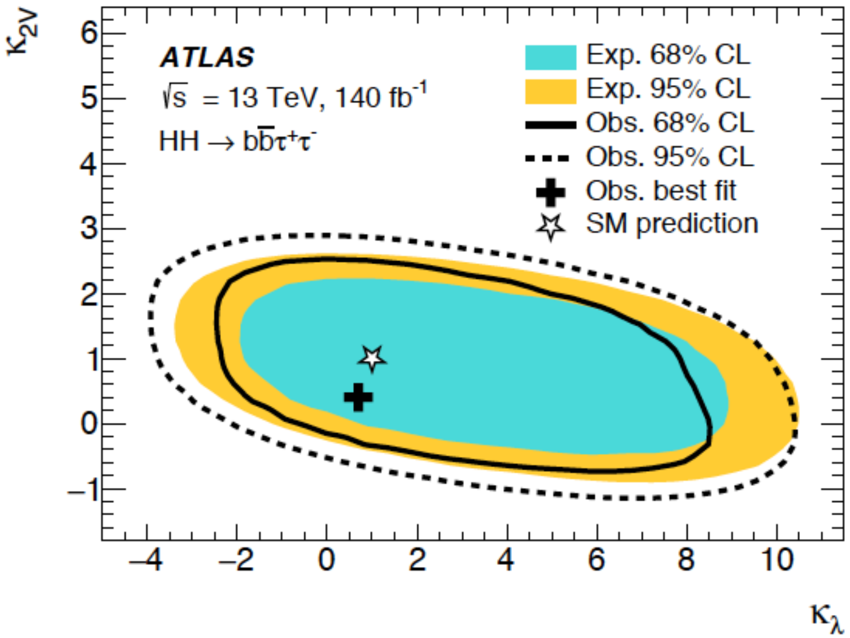

Figure 9: Likelihood contours at 68% (solid line) and 95% (dashed line) CL in the $(\kappa_\lambda, \kappa_{2V})$ parameter space, when all other coupling modifiers are fixed to one. The corresponding expected contours are shown by the inner and outer shaded regions. The SM prediction is indicated by the star, while the best-fit value is denoted by the black cross.

Boosted HH→bbbb

arXiv:2404.17193
24-April-2024

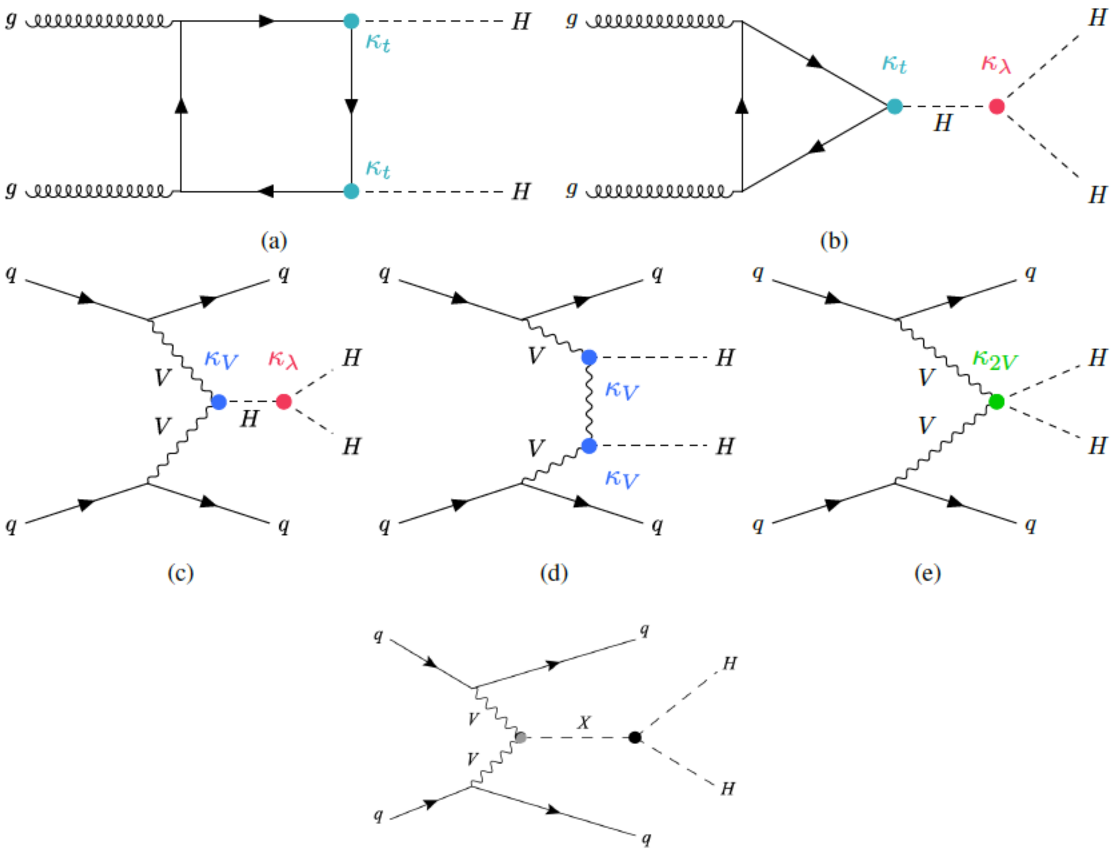

Boosted HH→bbbb

arXiv:2404.17193
24-April-2024

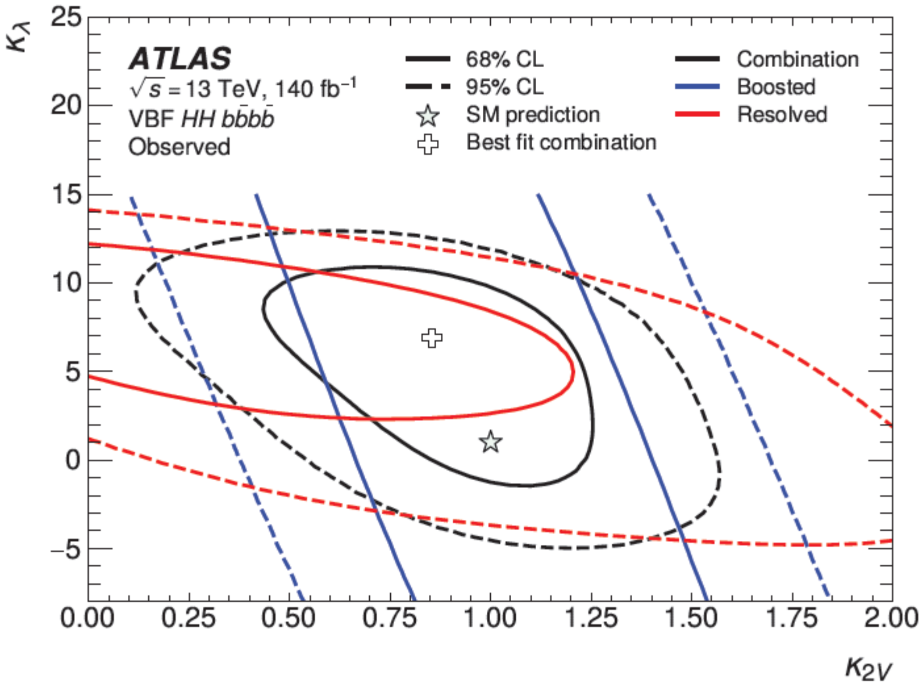

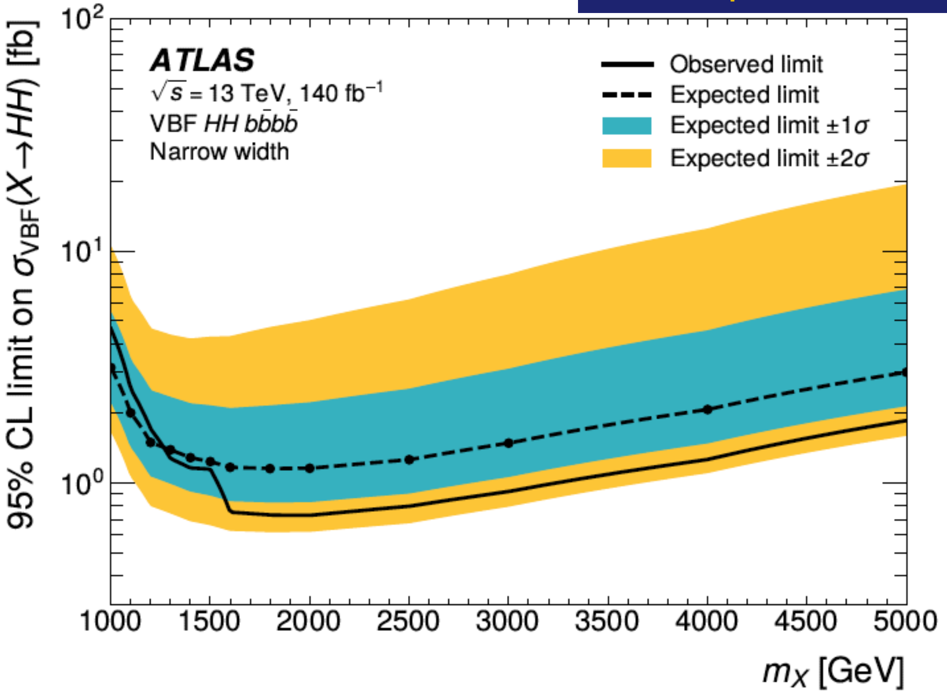

V+HH→bbbb (CMS)

arXiv:2404.08462
12-April-2024

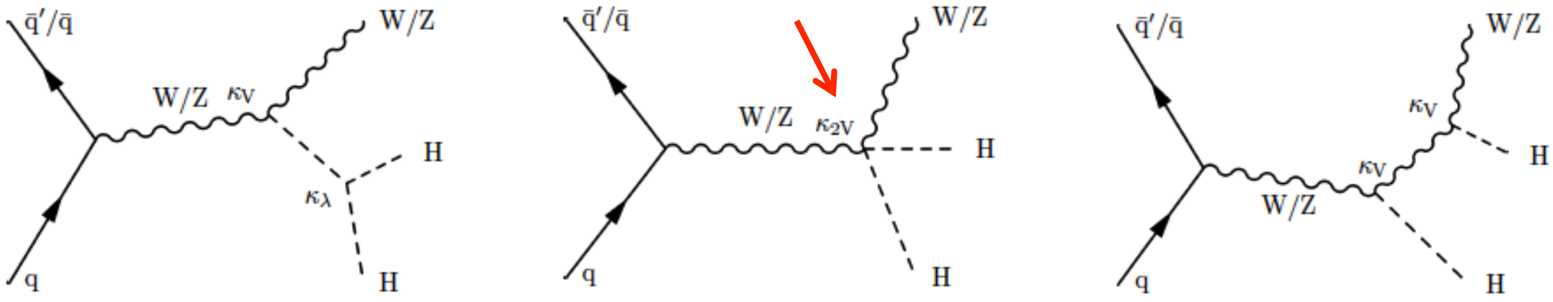

Table 1: The cross sections and uncertainties of different HH production modes [11–14], where PDF is the parton distribution function, α_S is the strong coupling constant, and m_t is the top quark mass.

Production mode	Cross section (fb)	Scale uncertainty	PDF+α_S uncertainty	m_t uncertainty
ggF	31.05	+2.2%/−5.0%	±3%	+4%/−18%
VBF	1.726	+0.03%/−0.04%	±2.1%	—
ZHH	0.363	+3.4%/−2.7%	±1.9%	—
W^+HH	0.329	+0.32%/−0.41%	±2.2%	—
W^-HH	0.173	+1.2%/−1.3%	±2.8%	—
$t\bar{t}$HH	0.775	+1.5%/−4.3%	±3.2%	—

V+HH→bbbb (CMS)

arXiv:2404.08462
12-April-2024

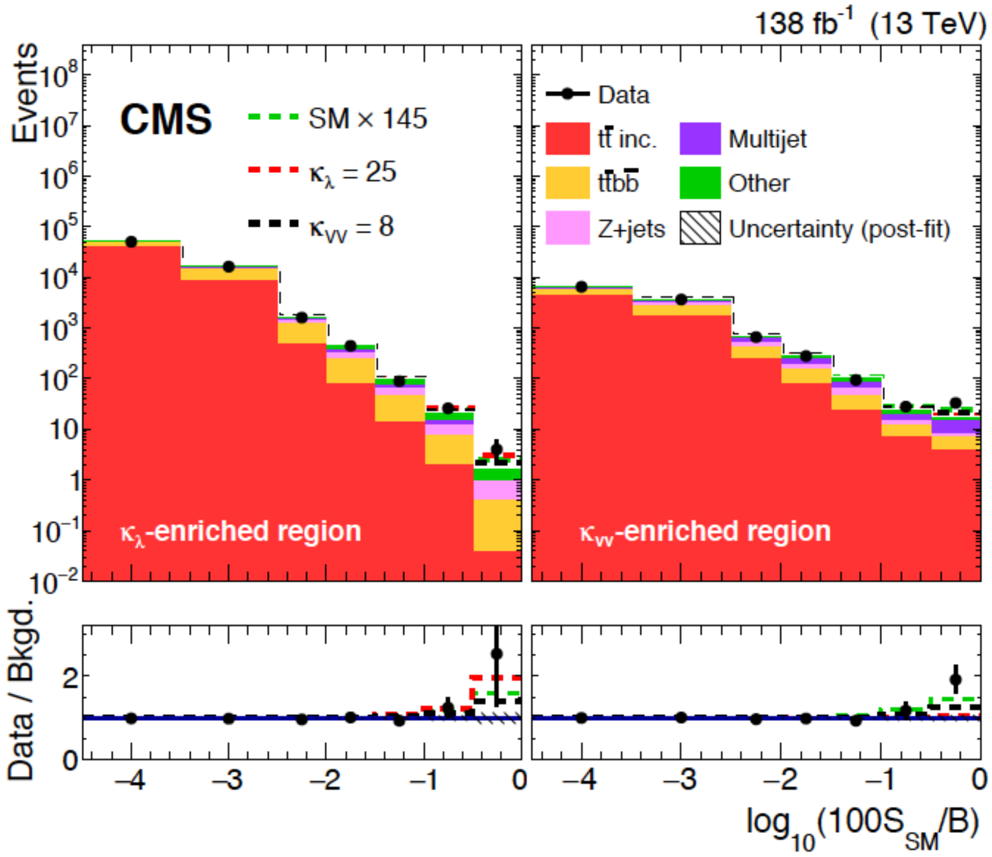

Small
Excess?

Searches for Dark Sectors (CMS)

arXiv:2405.13778
22-May-2024

Simplified dark sectors

Spin-1 portal

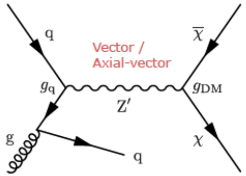

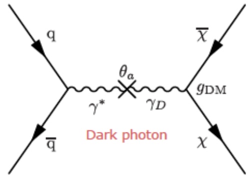

Spin-0 portal

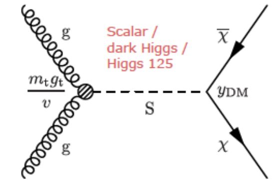

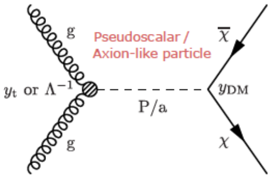

Extended dark sectors

2HDM+a

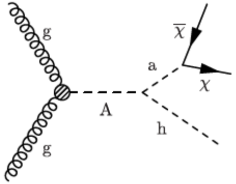

Stealth SUSY

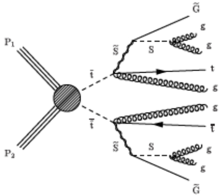

Hidden valleys

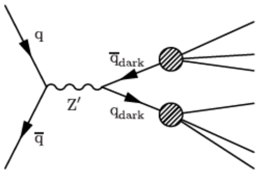

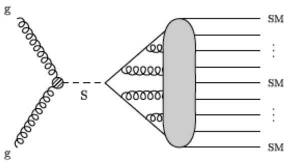

Long-Lived particles
Displaced vertices
Highly ionizing particles
etc. are all here!

Fermion portal

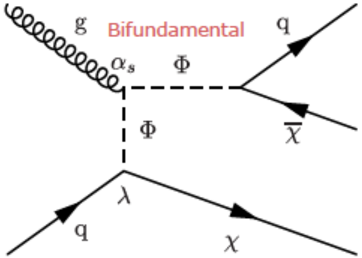

Inelastic Dark Matter

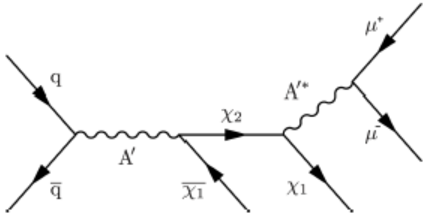

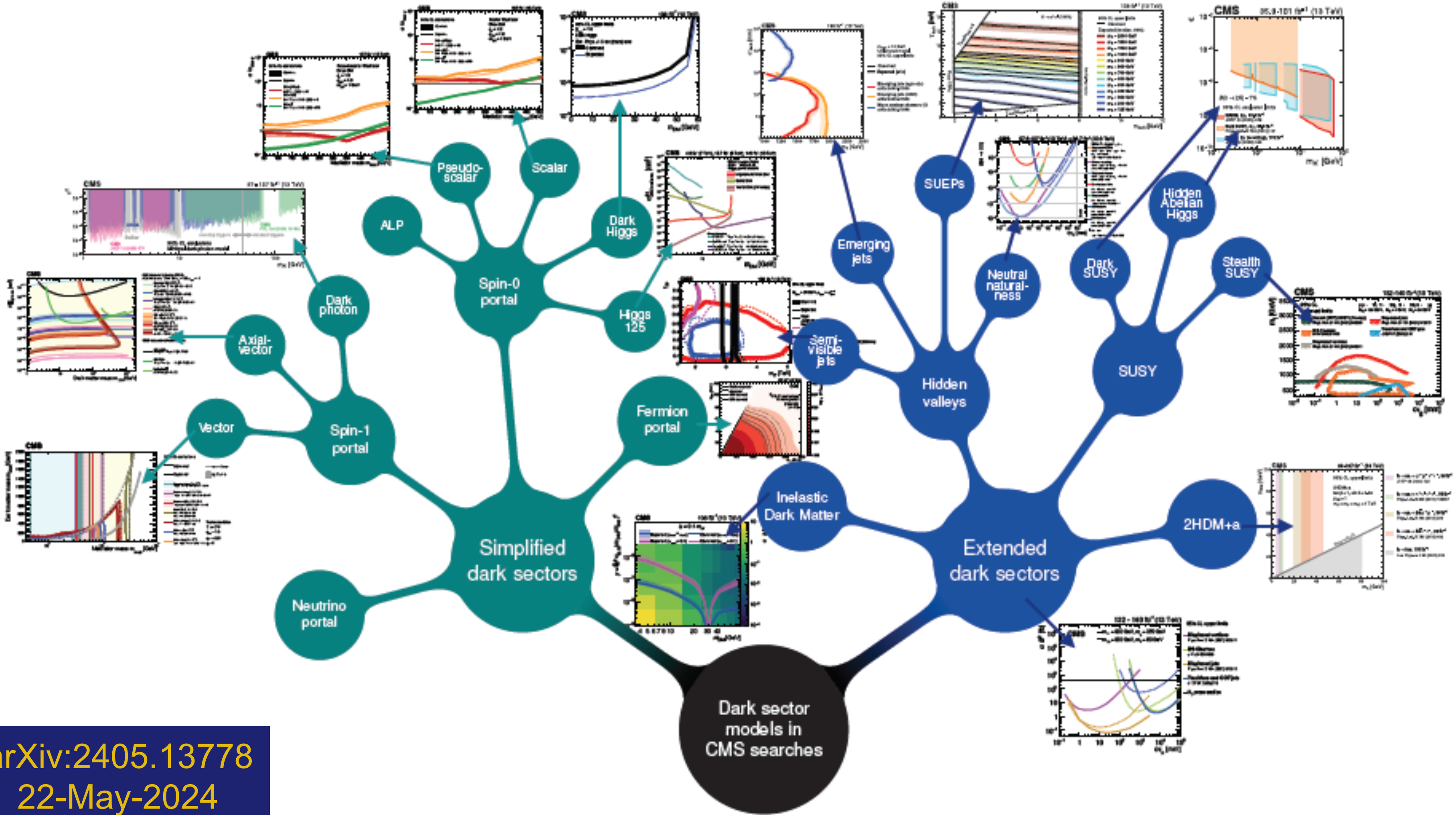

arXiv:2405.13778
22-May-2024

Run3, HL-LHC: accessing few-TeV masses

Many models, lots of data.
Looking for anomalies in scattering amplitudes.

Quest for new spectra ρ(m^2)

LHC high mass data: how do we constrain new physics (beyond SMEFT)

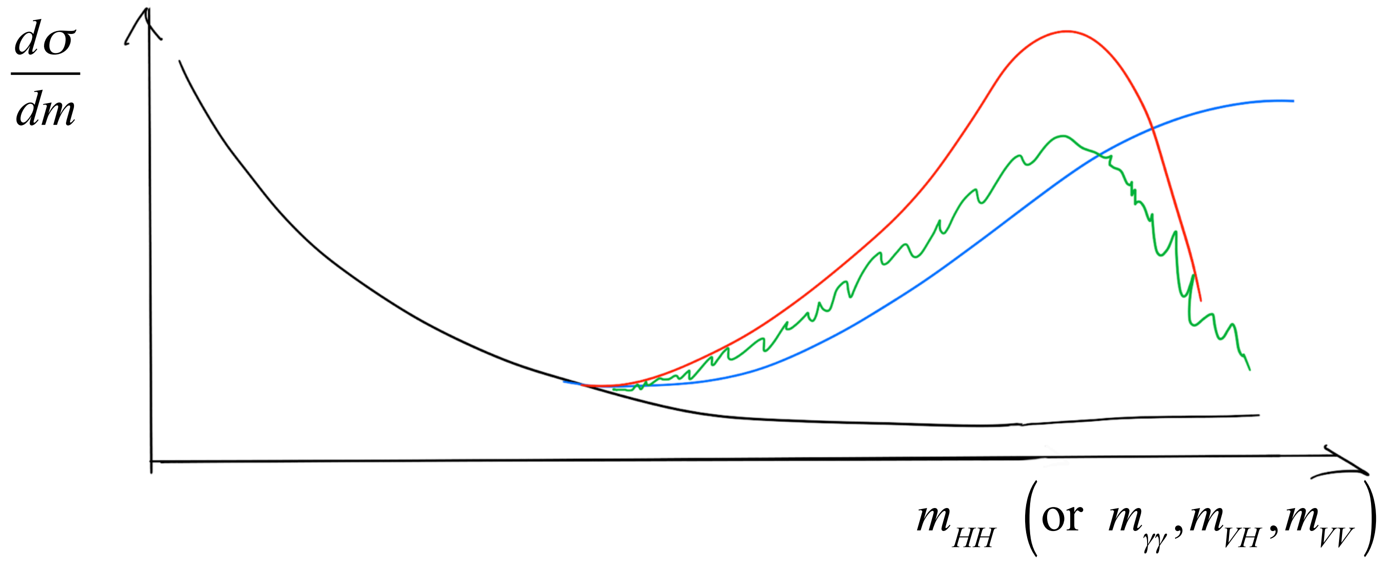

Example: heavy e^+e^- , γγ resonances

JHEP 10 (2023) 079

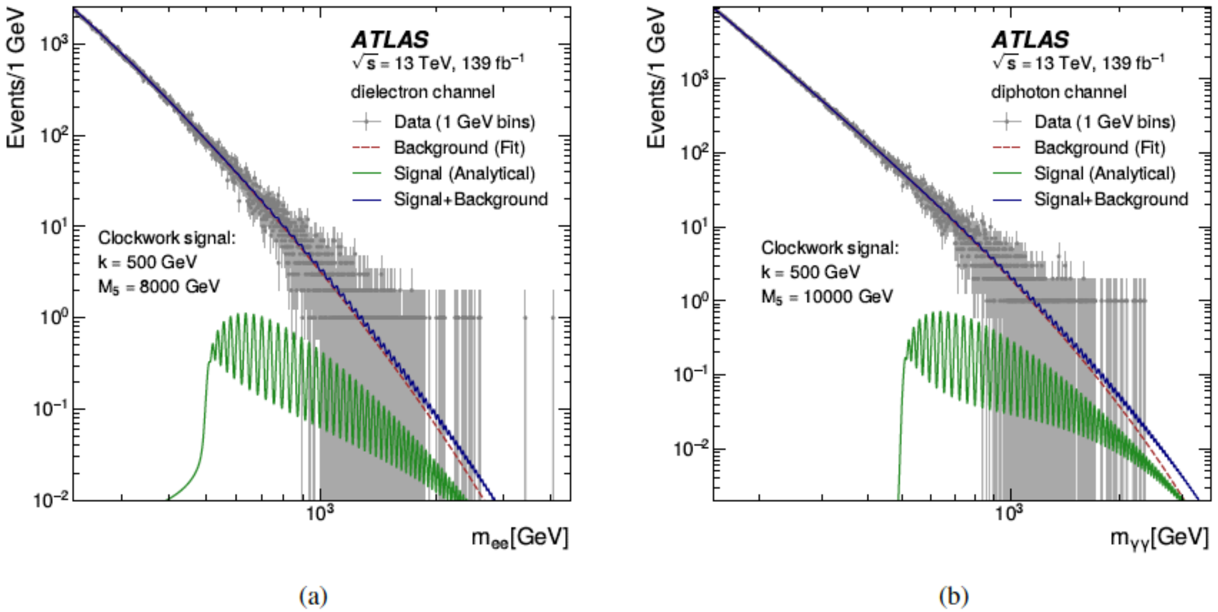

Figure 2: (a) The dielectron and (b) diphoton invariant mass distributions for events passing the full event selection, with the respective background-only fit parameterisation, an analytical clockwork signal, and the signal-plus-background parametrisation. The clockwork signal parameters are selected close to the sensitivity limit of this analysis. For the dielectron channel in (a) the clockwork signal is given for $k = 500$ GeV and $M_5 = 8000$ GeV, while the diphoton channel in (b) shows a signal with $k = 500$ GeV and $M_5 = 10000$ GeV.

Källén-Lehman representation

Following: Banks (Cambridge), McCullough (CERN) arXiv:2009.12399

$$L_{\text{int}} = \lambda O_{SM}(x) O_{NP}(x)$$

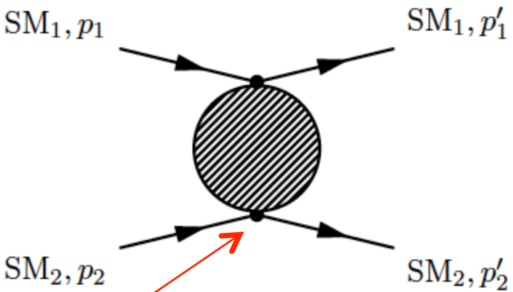

Two-point correlation function Δ(q) represented by the shaded area.
Factorize:

- external lines (SM particles), and
- interaction shaded region (SM+BSM)

$$\langle O_{NP}(x) O_{NP}(y) \rangle$$

$$\Delta(q) = \int_0^\infty dm^2 \rho(m^2) \frac{1}{q^2 - m^2 + i\varepsilon}$$

T-ordered 2-point correlation function

Spectral density function

$$\rho_{O_{NP}}(m^2) = (2\pi)^3 \sum_n \langle 0 | O_{NP} | n \rangle \langle n | O_{NP} | 0 \rangle \delta^{(4)}(m^2 - m_n^2)$$

Example: just a Higgs pole

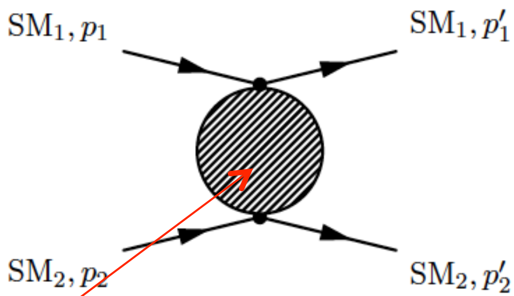

$$\Delta(q) = \int_0^\infty dm^2 \rho(m^2) \frac{1}{q^2 - m^2 + i\varepsilon} =$$

$$\Delta(q) = \int_0^\infty dm^2 \delta(m^2 = m^2_{Higgs}) \frac{1}{q^2 - m^2 + i\varepsilon} = \frac{1}{q^2 - m^2_{Higgs} + i\varepsilon}$$

Spectral density

Higgs propagator

… results in the Yukawa potential

Banks (Cambridge) McCullough (CERN) arXiv:2009.12399

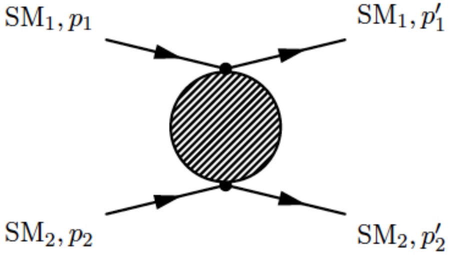

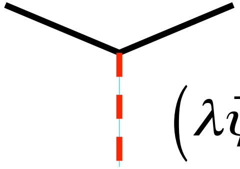

$$\left(\lambda\bar{\psi}\psi\Phi\right)^2$$

$$\Delta\left(q\right)=\frac{1}{q^2-m^2+i\varepsilon}\xrightarrow{p^2<<M_f^2}-\frac{1}{m^2+\left|q\right|^2}$$

$$i\boldsymbol{M}^{NR}=-i4M_f^2\lambda^2\delta^{s_1s_1'}\delta^{s_2s_2'}\Delta\left(q\right)$$

Insert K-L (the NR limit) in V(r):

$$V(r)=-\frac{1}{4M_f^2}\int\frac{d^3q}{\left(2\pi\right)^3}\boldsymbol{M}^{NR}e^{i\vec{q}\vec{r}}=-\frac{\lambda^2}{4\pi}\frac{e^{-mr}}{r}$$

Yukawa

So, for any spectral density ρ(m²):

$$V(r)=-\frac{\lambda^2}{4\pi r}\int dm^2\rho\left(m^2\right)e^{-mr}$$

Yukawa for a whole spectrum of exchanged states

Nonlocalizable theories and $\rho(m^2)$

SP: arXiv:2404.09159 14-April-2024

Biswas, Okada: NPB 898 (2015) 113-131
Buoninfante et.al. PRD 101 (2020) 8, 084019

Nonlocalizable theories

The growth of spectral densities with m^2 provides info on the localizability of the theory

$$\rho\left(m^2\right) = e^{m^{2a}} \times \text{ subdominant terms}$$

- $a < 1/2$ theory strictly localizable
- $a = 1/2$ theory quasi-local
- $a > 1/2$ theory nonlocalizable

Why nonlocality

arXiv:2009.10856
Jens Boos

$$\nabla^2 \phi(r) = 4\pi G m \delta(r) \quad \Rightarrow \quad \phi(r) = -\frac{Gm}{r}$$

Potential is singular at r=0.
Regularize the potential by introducing a heavy scale M:

$$\nabla^2 \left(1 - \frac{\nabla^2}{M^2}\right) \phi(r) = 4\pi G m \delta(r) \quad \Rightarrow \quad \phi_{reg}(r) = -\frac{Gm}{r}\left(1 - e^{-Mr}\right)$$

Field finite at r=0, but field derivative also not zero at r=0.
Can add more scales.
However, the propagator has negative mass poles (ghosts).

Why nonlocality

Potential is singular at r=0.
Regularize the potential by introducing a heavy scale M:

$$\nabla^2 e^{-\frac{\nabla^2}{M^2}}\phi(r) = 4\pi Gm\delta(r) \quad \Rightarrow \quad \phi_{reg}(r) = -\frac{Gm}{r}\mathrm{erf}\left(\frac{Mr}{2}\right)$$

This is equivalent to smearing the point-like interaction to a Gaussian.

$$\nabla^2\phi(r) = 4\pi Gm\underbrace{e^{\frac{\nabla^2}{M^2}}\delta(r)}$$

- No ghosts at tree level.
- Non-local: information from infinite distance from r is needed.
- No infinities
- Others

Fine structure: the Darwin term

It may come as a surprise, although an interpretation,

$$H = H_0 - \frac{p^4}{8m^3c^2} + \frac{1}{2m^2c^2}\frac{1}{r}\frac{\partial U}{\partial r}\vec{S}\vec{L} + \underbrace{\frac{1}{8}\frac{\hbar^2}{m^2c^2}}\nabla^2 U$$

Gaussian smearing the electron position at r=0 by ~ its Compton length r_{NL}:

$$\nabla^2 e^{\frac{r_{NL}^2}{2}\nabla^2} U(r) = 4\pi e^2 \rho(r) \quad \Rightarrow \quad \nabla^2\left(1 + \underbrace{\frac{1}{8}\frac{\hbar^2}{m^2c^2}}\nabla^2 + \cdots\right) U(r) = 4\pi e^2 \rho(r)$$

Nonlocality at the eweak scale

$$\mathcal{A} = \int d^4x \left[-\frac{1}{2} \phi e^{\frac{\Box}{\Lambda_{NL}^2}} \left(\Box + m_\phi^2 \right) \phi - V(\phi) \right]. \qquad (3)$$

Employing a $(+,-,-,-)$ metric, $p^2 = -\Box$, the propagator is given by [22]:

$$\Delta\left(p^2\right) = \frac{e^{p^2/\Lambda_{NL}^2}}{p^2 - m_\phi^2 + i\epsilon}. \qquad (4)$$

Question: can we motivated such FFs ?

Usual problem: we typically expect nonlocality to kick in at scales close to Planck. How do we create a hierarchy?

$$\sigma_{NL-SM} = e^{a\frac{s}{\Lambda_{NL}^2}} \times \sigma_{SM}$$

Adhoc modification to constrain using sqrt(s)>TeV data.

Biswas, Okada: NPB 898 (2015) 113-131

Buoninfante et.al. PRD 101 (2020) 8, 084019

Example: string scattering

Infinite derivative operators well known in String Theory:

$$V = e^{c\frac{\Box}{M_s^2}}$$

String Tension (used in ST vertices)
Scale of non-locality

$$a' = \frac{1}{M_s^2}$$

Universal Regge Slope
(back at the 60's!)

Regge trajectory $a'E^2 = N\hbar$

For QCD strings $a' = \left(10^{-15}\ \text{m}\right)^2$

For super strings $a' = \left(10^{-33}\ \text{m}\right)^2$

EPJ A 48, 127 (2012)

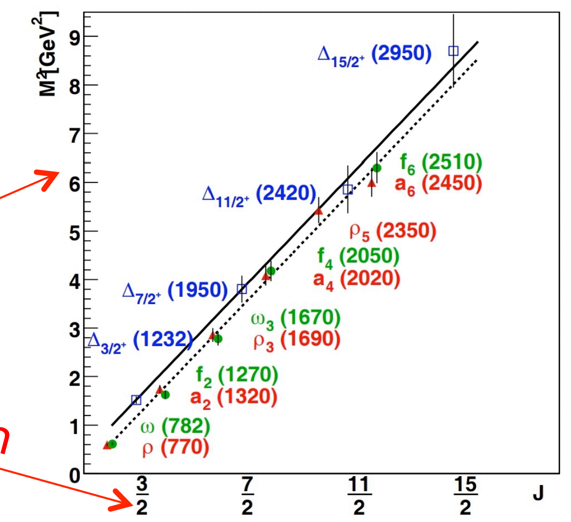

Fig. 1. The leading Regge trajectory: Δ resonances with maximal J in a given mass range. Also shown is the Regge trajectory for mesons with $J = L + S$.

Nonlocality at the eweak scale

$$\mathcal{L}_{\text{eff}} = \mathcal{L}_{\text{ren}} + \sum_{n=d}^{\infty} \frac{\mathcal{O}_n}{M_p^{n-d}}$$

EFTs: a sum of renormalizable ops and a tower of non-renormalizable terms obtained after integrating out UV DOF's

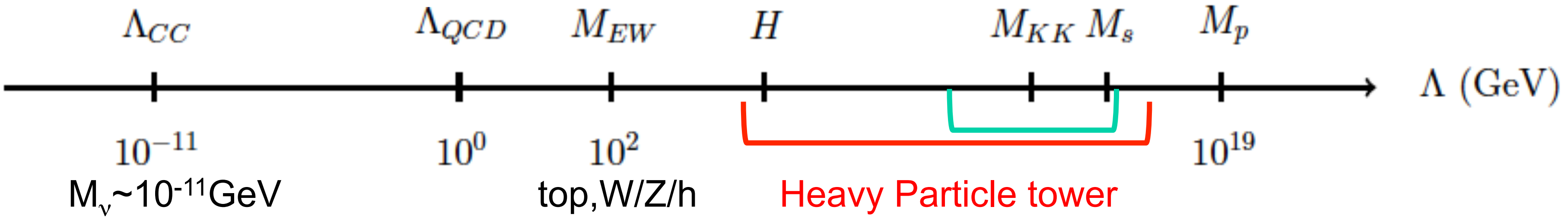

- At lower energy scales UV effects have been integrated out.
- As we increase the scale $\Lambda \rightarrow \Lambda_{NP}$, the effect of the tower states gets larger and higher dim operators O_n in the OPE blow up.
- Note there could be hierarchies between the lightest state and Λ_{NP}.
- **We proposed an early BSM probe: High Pt Higgs**

Li, Nicolaidou, SP, EPJC, arXiv:1904.03995 (2019)

Hoffmann, Kaminska, Nicolaidou, SP, EPJC74 (2014) 3181

Heavy Particle Towers at Λ_{BSM}

Typical spectrum of an interacting QFT

Callum Robert King Thesis on spectral densities.

$$\rho\left(m^2\right) = e^{m^2 a}$$

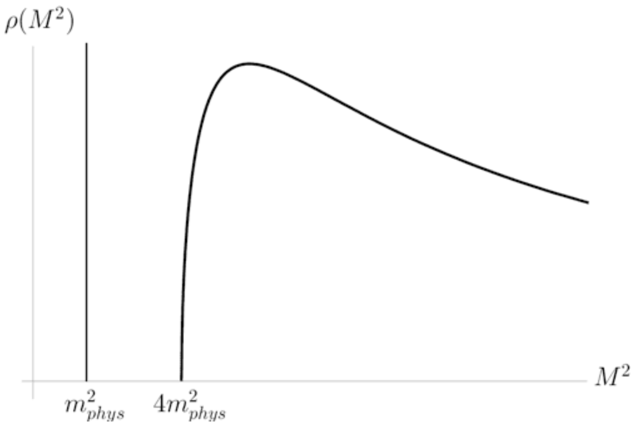

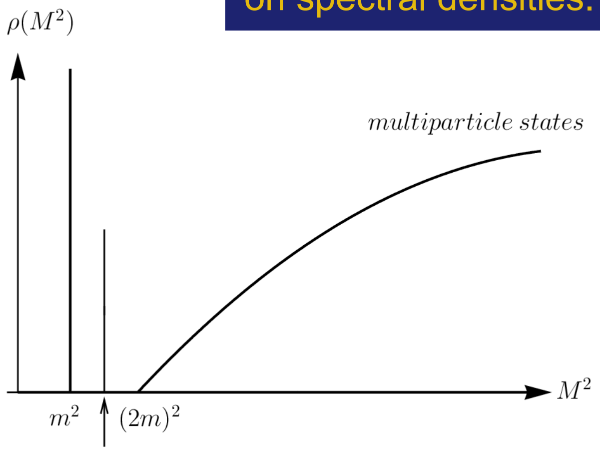

$$\Delta\left(q\right) = \int_0^\infty dm^2 \rho\left(m^2\right) \frac{1}{q^2 - m^2 + i\varepsilon}$$

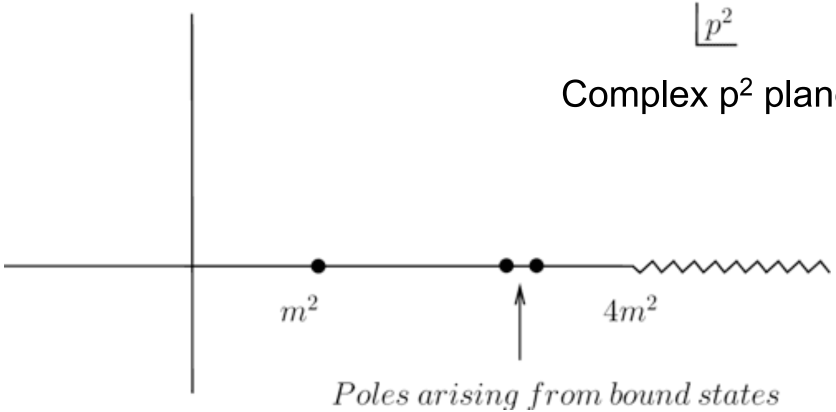

Complex p^2 plane

spectral densities from 2-pt CFs

2-pt function →

$$\Delta(p) = \int_0^\infty dm^2 \rho(m^2) \frac{1}{p^2 - m^2 + i\varepsilon} = -\frac{1}{\pi}\int_0^\infty dm^2 \frac{\mathrm{Im}\left[\Delta(m^2)\right]}{p^2 - m^2 + i\varepsilon}$$

From spectral density →

$$\rho(p^2) = -\frac{1}{\pi}\mathrm{Im}\left[\Delta(p^2)\right] = \frac{1}{\pi}\mathrm{Im}\left[\mathcal{M}(\mathcal{A}\to\mathcal{A})\right] \Rightarrow$$

$$\rho(p^2) = \sum_{X_n}\int d\Pi_{X_n}\left|\mathcal{M}(\mathcal{A}\to X_n)\right|^2 (2\pi)^3 \delta^4\left(p_{\mathcal{A}} - p_{X_n}\right)$$

Using Optical Theorem to get the fwd Ampl $\mathcal{M}$

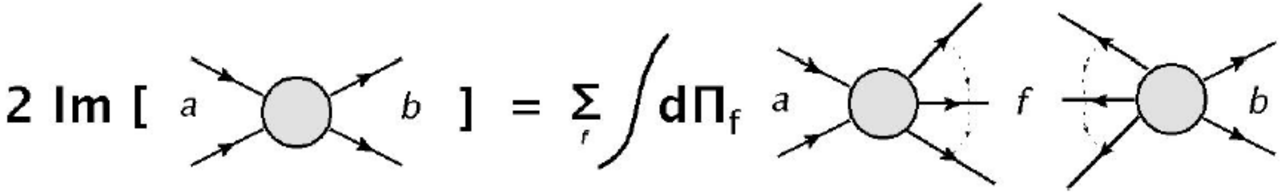

hh scattering: exchange of n scalars

SP: arXiv:2404.09159
14-April-2024

$$\mathcal{M}\left(hh \to \phi^n\right) = n!$$

$$\rho_n\left(p^2\right) = \frac{\left(n!\right)^2}{2\pi}\frac{1}{n!}\left[\int d\Pi_{X_n}\left(2\pi\right)^4 \delta^4\left(m - \sum_i^n p_i\right)\right] = \frac{n!}{2\pi} I_n$$

$$\rho\left(p^2\right) = \sum_i^n \rho_i\left(p^2\right) \xrightarrow{n\to\infty} \sqrt{2\pi n}\left(\frac{n}{e}\right)^n \approx e^{n\ln(n)}$$

$$e^{\frac{p}{m}} < \rho\left(p^2\right) < e^{\frac{p^2}{m^2}}$$

In what follows we will assume that the large degeneracy of intermediate states leads to an exp rising spectral density as follows:

$$\rho\left(p^2\right) \approx e^{\frac{p^2}{\Lambda_{NL}^2}}$$

$$\Lambda_{BSM}^2 = \Lambda_{NL}^2$$

Here the BSM scale is the nonlocality scale

NL Klein-Gordon propagator

$$\Delta(p)=\int_0^\infty dm^2\rho(m^2)\frac{1}{p^2-m^2+i\varepsilon}\xrightarrow{p^2>>m^2}\frac{e^{\frac{p^2}{\Lambda_{NL}^2}}}{p^2-m^2+i\varepsilon}$$

NL Klein-Gordon Propagator

This is the same propagator as the one obtained from the Non-Local Lagrangian:

$$L=-\phi(x)e^{\frac{\partial_\mu\partial^\mu}{\Lambda_{NL}^2}}\left(\partial_\mu\partial^\mu+m_h^2\right)\phi(x)\ -V(\phi)$$

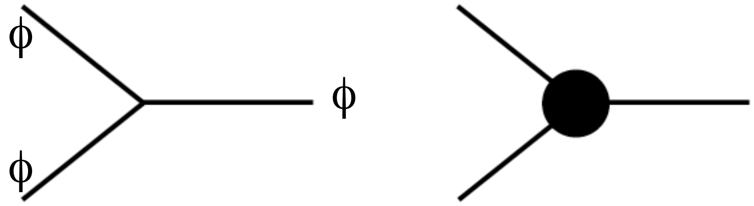

Local vertex

Nonlocal vertex

For $p^2<<\Lambda^2$ vertices look point-like

Generalize

SP: arXiv:2404.09159
14-April-2024

D. Nonlocal Källèn-Lehmann Representation

In the case of a nonlocalizable theory, the KL representation can be written using the spectral density $\rho(m^2)$ in an integral representation with non-local propagators:

$$\Delta\left(p^2\right) = \int_0^\infty \frac{\mathcal{F}(p^2 - m^2)\rho\left(m^2\right)}{p^2 - m^2 + i\epsilon} dm^2 \tag{33}$$

$$= \int_0^\infty \frac{e^{\frac{p^2 - m^2}{\Lambda_{NL}^2}} \rho\left(m^2\right)}{p^2 - m^2 + i\epsilon} dm^2. \tag{34}$$

New Result
(without proof)

The IR limit of this definition of the KL, approaches Eq. 32.

New paper appeared: 'Form factors, spectral and Källén-Lehman representation in nonlocal quantum gravity', Briscese et.al. arXiv:2405.1405 (24-May-2024)

SM Phenomenology

Motivated by the hierarchy problem [1], a number of extensions of the standard model (SM) of particle physics introduce new-physics scales, $\Lambda \sim \mathcal{O}(\text{TeV})$, with characteristic signature the presence of new states or towers of states close to that scale. Such heavy particle towers (HT) are assumed to couple to the SM particles and are also expected to have their lightest state at a mass of order $m_1 \sim \Lambda$. Examples are large extra spatial dimension models like the ones proposed by ADD, [2], and RS, [3], where Kaluza-Klein (KK) modes of the graviton that couple to the SM appear. In other models, [4], an infinite tower of massive spin-2 graviton KK modes is predicted. The HT modes in these models could be closely spaced leading to a sequence of resonances or a non-resonant continuum excess in the measured diphoton spectrum at high masses at the LHC [5, 6]. It should be noted that non-gravitational models can also lead to particle towers, as is the case of composite Higgs models where towers of new, heavy-quark bound states are predicted [7].

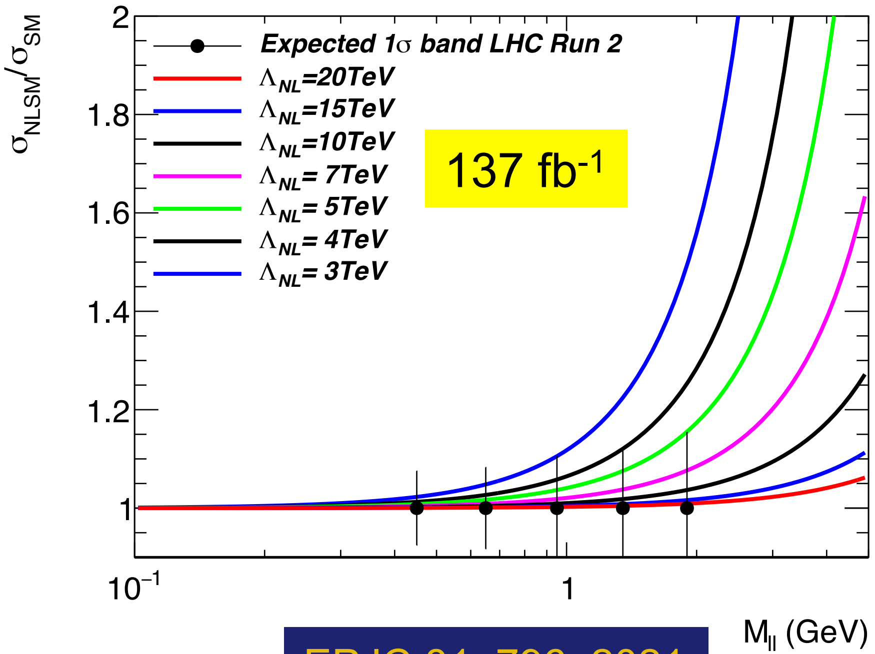

EPJC 81, 796, 2021

$$\sigma_{NL-SM} = e^{a\frac{s}{\Lambda_{NL}^2}} \times \sigma_{SM}$$

VBF di-Higgs very sensitive to BSM

EPJC (2017) 77:481

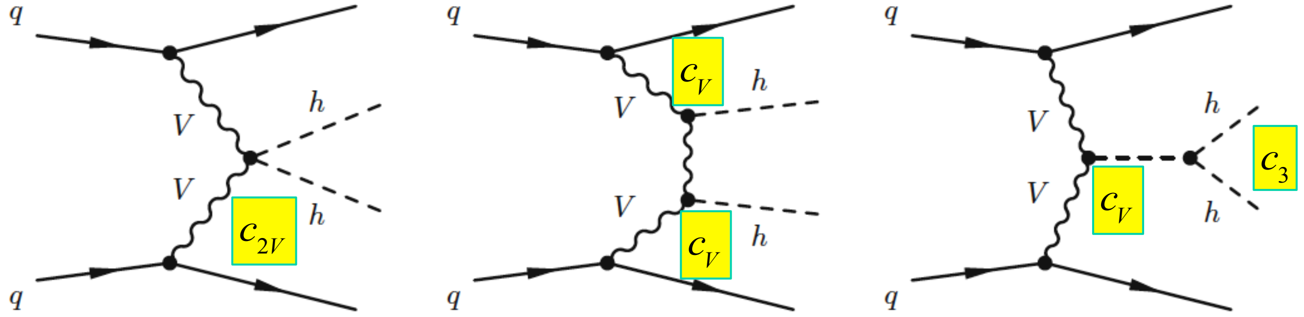

Fig. 1 Tree-level Feynman diagrams contributing to Higgs pair production via VBF. In terms of Eq. (2), the *left*, *middle*, and *right diagrams* scale with c_{2V}, c_V^2, and $c_V c_3$, respectively

In the SM:

$$c_{2V} = 1$$
$$c_V = 1$$
$$c_3 = c_4 = 1$$

$$\mathscr{A}(V_L V_L \to hh) \simeq \frac{\hat{s}}{v^2}(c_{2V} - c_V^2),$$

up to $\mathcal{O}(m_W^2/\hat{s})$ and $\mathcal{O}(\hat{s}/\Lambda^2)$ corrections.

In SM we have a cancellation between the first and the second diagrams.

For new BSM towers the amplitude is modified and destructive interference is lifted:

$$\mathcal{A}(V_L V_L \to hh) \simeq \frac{s}{v^2}\left(e^{\frac{s}{\Lambda^2_{NL}}} - 1\right)$$

Can we cleanly measure this?

- Use HG Calorimeter + tracker to tag/trigger most of the VVHH events.
- High acceptance for VBS: VV→VV
- Improve VBF measurements.

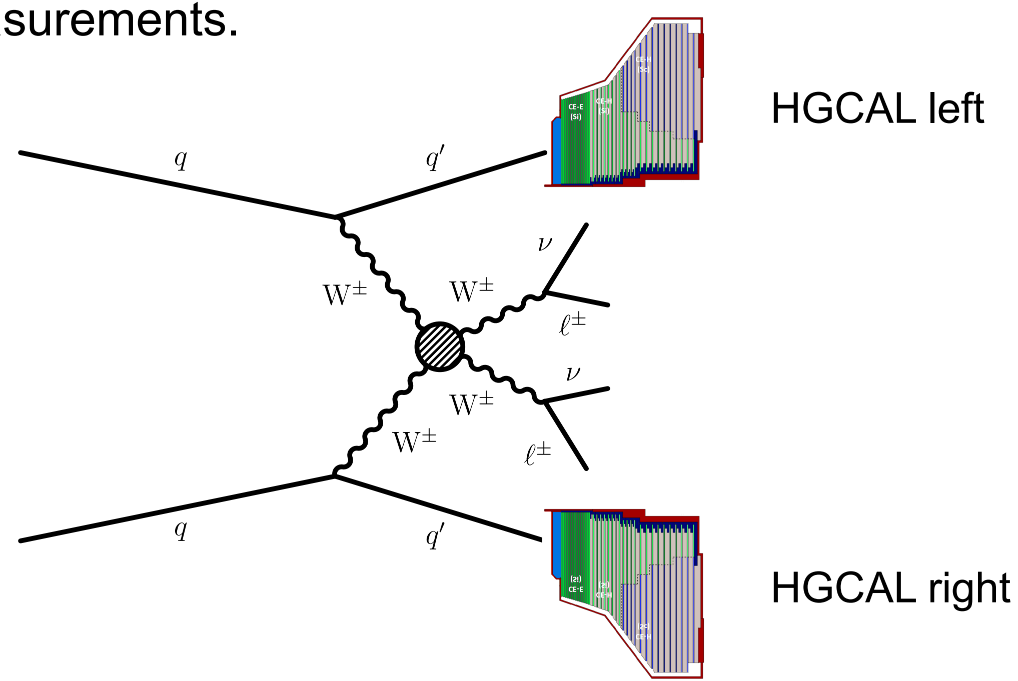

VBF angles smaller than VBS & HH

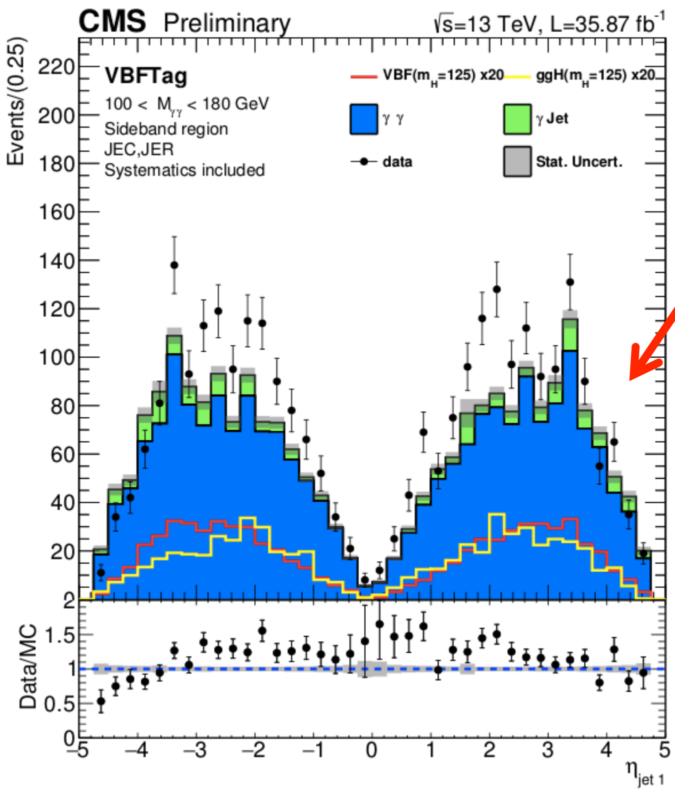

Bjorken x

$$\eta(\mathrm{VBF}) = a\cosh\left(\frac{P}{Q}\right) = a\cosh\left(\frac{P}{M_H/2}\right) = a\cosh\left(\frac{0.1\times 6.5\mathrm{TeV}}{0.063\mathrm{TeV}}\right) \sim 3$$

For di-Higgs the angle is larger:

$$\eta(\mathrm{HH}) = a\cosh\left(\frac{P}{M_H}\right) \sim 2.3$$

Quark jets go right in the center of HGCAL

CMS High Granularity Calorimeter (~miT)

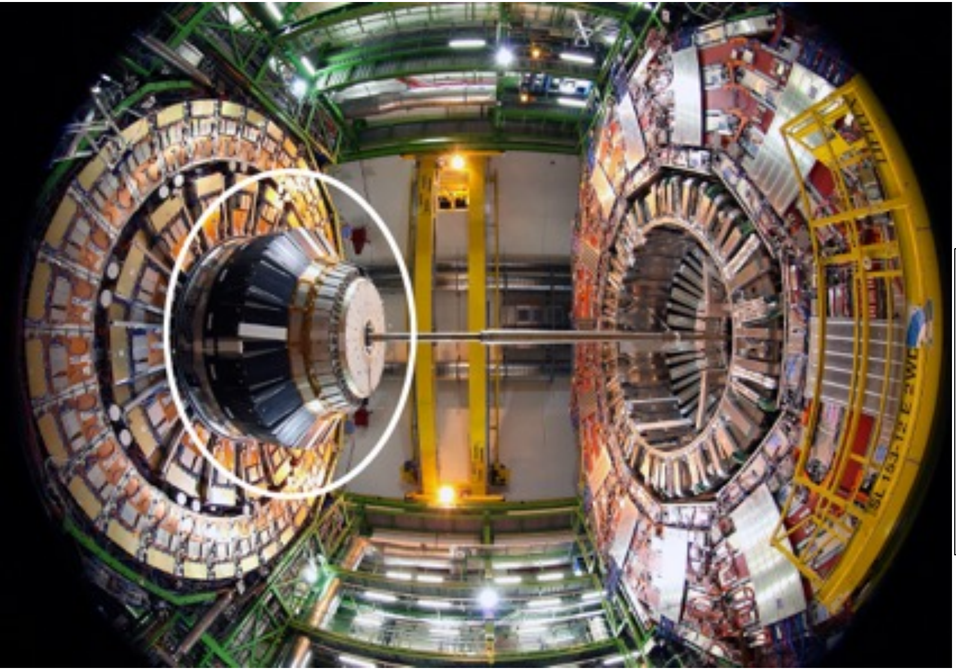

Active Elements:
- Hexagonal modules based on Si sensors in CE-E and high-radiation regions of CE-H
- "Cassettes": multiple modules mounted on cooling plates with electronics and absorbers
- Scintillating tiles with on-tile SiPM readout in low-radiation regions of CE-H

Key Parameters:
Coverage: $1.5 < |\eta| < 3.0$
~215 tonnes per endcap
Full system maintained at -30°C
~620m² Si sensors in ~26000 modules
~6M Si channels, 0.6 or 1.2cm² cell size
~370m² of scintillators in ~3700 boards
~240k scint. channels, 4-30cm² cell size
Power at end of HL-LHC:
~125 kW per endcap

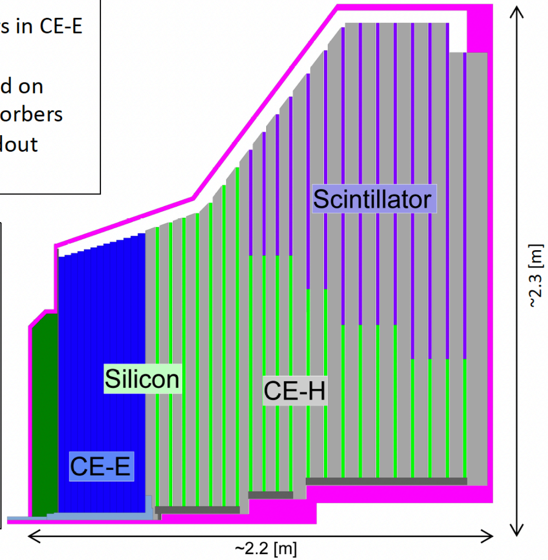

Electromagnetic calorimeter (**CE-E**): **Si**, Cu & CuW & Pb absorbers, 26 layers, 27.7 X_0 & ~1.5λ
Hadronic calorimeter (**CE-H**): **Si** & **scintillator**, steel absorbers, 21 layers, ~8.5λ

However, Phase-2 is still far (2029) → keep analyzing the Run-3 data.

Summary

- LHC Run 3 started in 2022: experiments trying to find cracks in the SM

- Non-local (like) effects are an interesting possibility:
  - Can generalize local spectral representations of BSM operators and test directly against data.

- **Non-locality in QM and Gravity** and applications is an open field
  - How do we regularize non-local 2pt functions?

- Di-Higgs, VB Fusion and VB Scattering are key processes for testing the SM.

Extra Slides

Heavy diphoton continuum

arXiv:2405.09320 (15 May 2024)

Hsin-Yeh Wu PhD

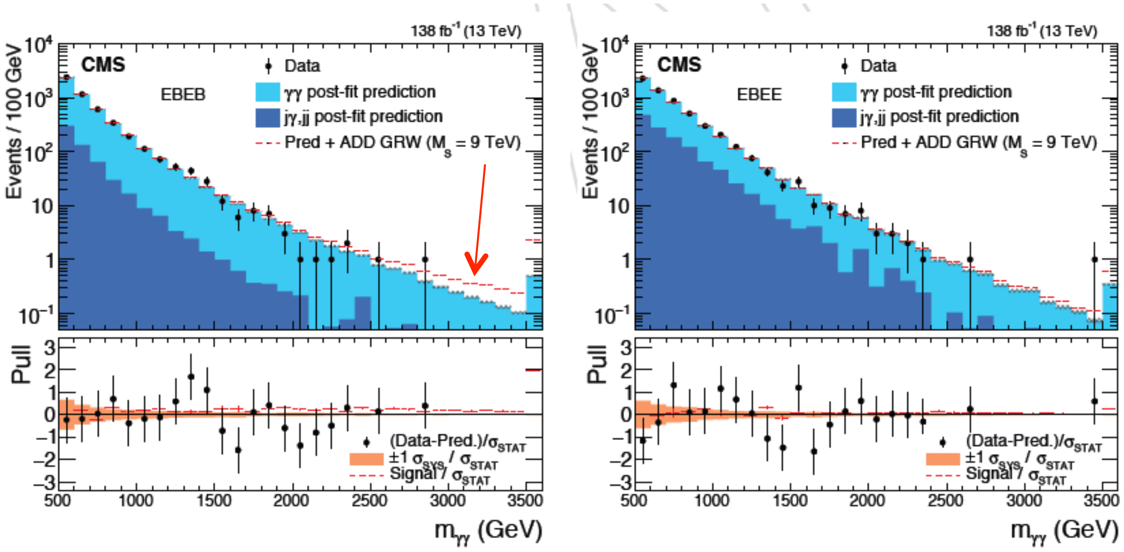

Figure 6: The $m_{\gamma\gamma}$ spectra and background prediction after nuisance parameter marginalization ("post-fit") due to SM diphoton production ($\gamma\gamma$) and misidentified photon production (jγ, jj) for the EBEB (left) and EBEE (right) cases, combining the 2016, 2017, and 2018 data sets. The prediction with an ADD signal (GRW convention with $M_S = 6$ TeV) is also shown. The pull distributions, defined as the data minus prediction divided by the statistical uncertainty, are shown in the lower panel. The shaded bands show the systematic uncertainties, neglecting the normalization of the diphoton prediction. The last bin contains the overflow of events beyond $m_{\gamma\gamma} > 3.5$ TeV.

Warped extra dimensions

arXiv:2403.16926 (March 2024)

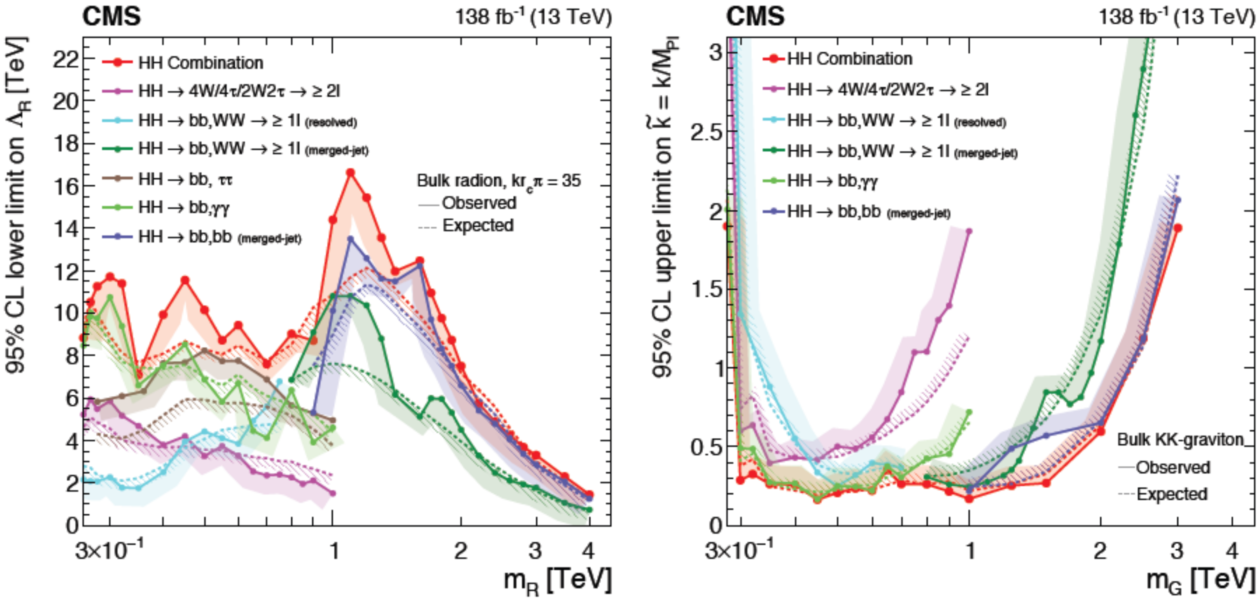

Figure 35: Observed and expected limits, at 95% CL, on the parameters of models with warped extra dimensions, as obtained from the X → HH analyses presented in this report and their combined likelihood analysis. Shown are lower limits (left) on the bulk radion ultraviolet cutoff parameter Λ_R, as a function of the radion mass m_R, and upper limits (right) on the parameter $\tilde{k}$ of the spin-2 bulk graviton G, as a function of m_G. Excluded areas are indicated by the direction of the hatching along the exclusion contours.

Search for X→HH→bbγγ

arXiv:2112.11876 (2022)

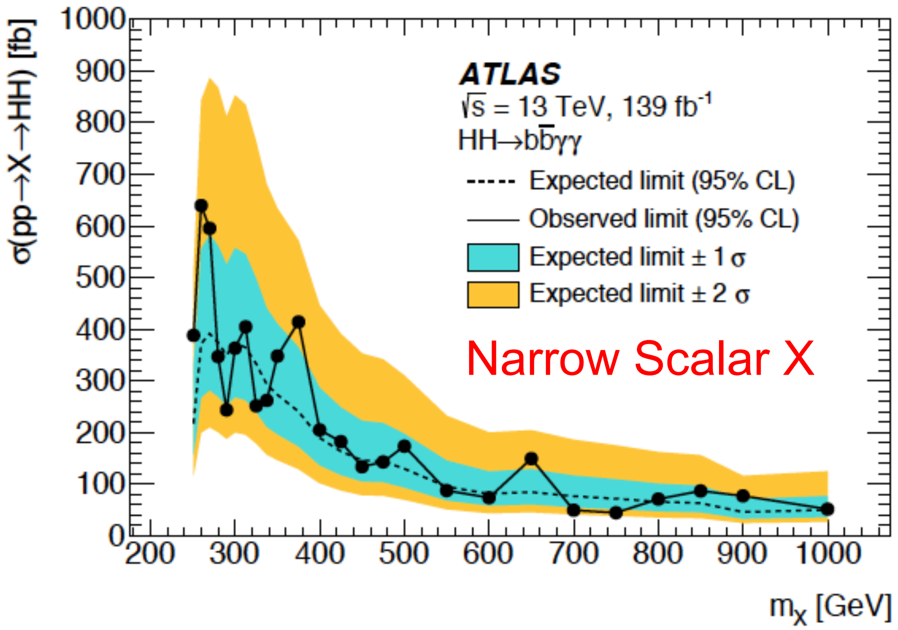

Figure 15: Observed and expected limits at 95% CL on the production cross section of a narrow-width scalar resonance X as a function of the mass m_X of the hypothetical scalar particle. The black solid line represents the observed upper limits. The dashed line represents the expected upper limits. The $\pm 1\sigma$ and $\pm 2\sigma$ variations about the expected limit due to statistical and systematic uncertainties are also shown.

HVT limits on g_H

arXiv:2403.16926 (March 2024)

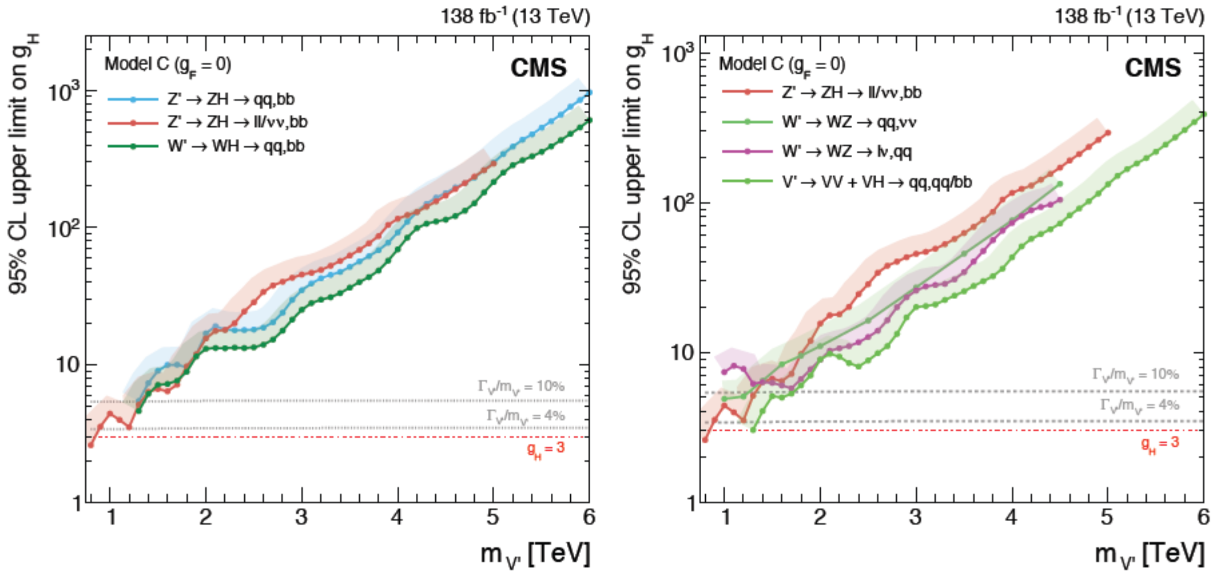

Figure 40: Obseved upper limits, at 95% CL, on the coupling g_H within the heavy vector triplet model, as a function of the V′ mass. The limits are shown for the vecotr boson fusion production mode in the context of model C, in which $g_F = 0$. The results are shown (left) for the WH and ZH analyses of Refs. [109–111], individually, and for a combination with the WZ final states of Refs. [109, 111, 196] (right), where the WH and ZH results from all-hadronic final states have been combined with the corresponding VV channels. The dotted lines denote coupling values above which the relative width of the resonance, $\Gamma_{V'}/m_{V'}$, exceeds 4 and 10%, respectively, implying the narrow width approximation no longer applies.

Continuing measurements in run 3

- Higgs and EW Precision:
  - Couplings, Mass & Width, Spin Parity, STXS & Differential, **W mass**, …
- New massive particles: new Higgs, new scalars, new vectors, Gravitons, Susy
  - Diphoton, Dilepton, Dijet FS, etc.
- Massive diboson final states: VV, VH, HH
  - Heavy Resonances
- Long-lived particles
- Effective Field Theory (EFT)
- B physics: CPV, CKM measurements, mixing, spectroscopy
- B anomalies related measurements

Categories overlap/correlate; classification helps keep track of various observables.

Impact: VBS and di-Higgs

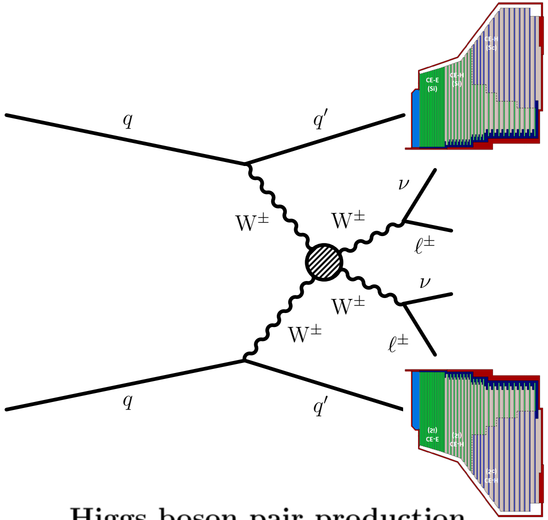

HGCAL left

HGCAL right

Higgs boson pair production

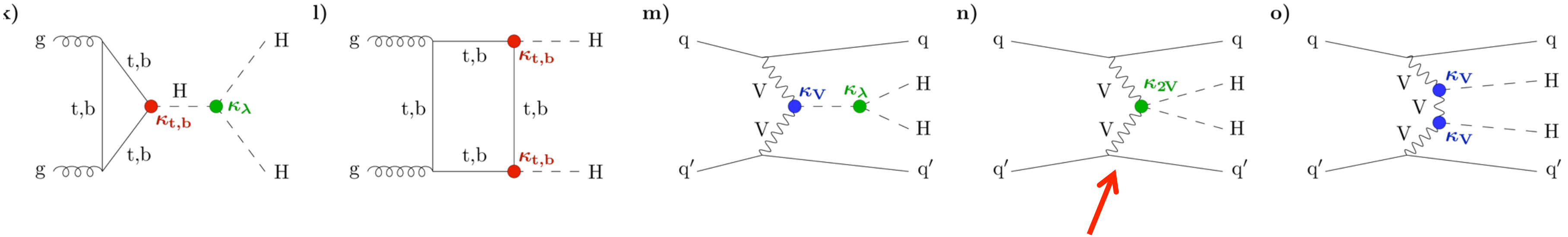

Note the unique tree-level VVHH
diagram that only appears in VBF mode

Higgs pair production

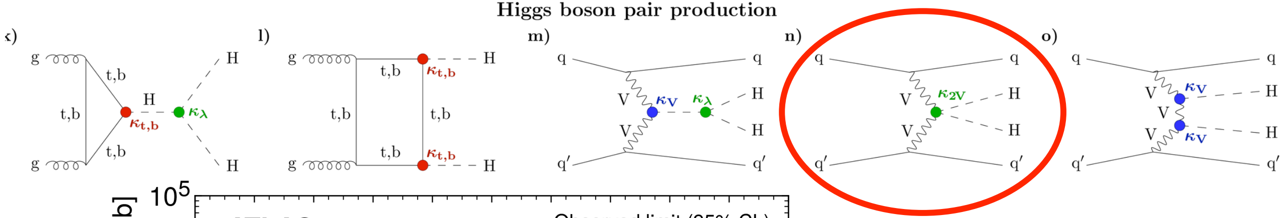

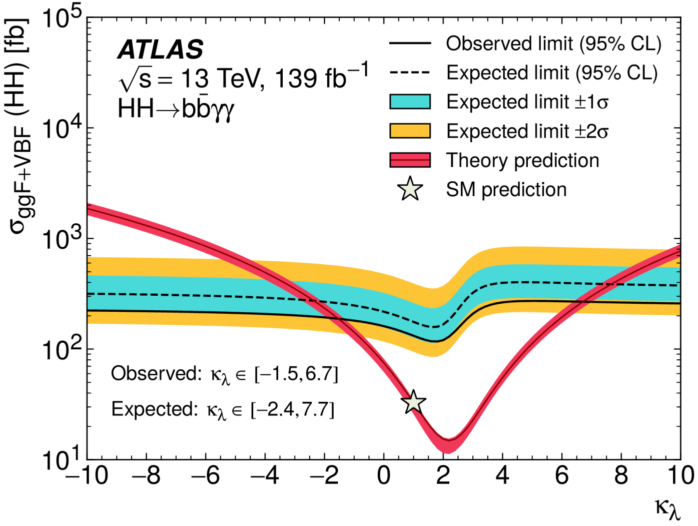

ATLAS-HDBS-2018-34

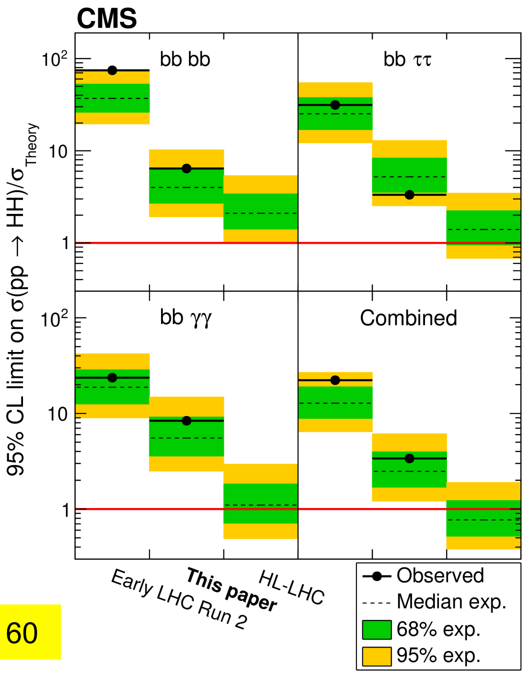

Nature 607 (2022) 60

Observed and expected limits at 95% CL on the cross section of **non-resonant Higgs-boson pair production** as a function of the Higgs-boson self-coupling modifier $\kappa_\lambda = \lambda_{HHH}/\lambda^{SM}_{HHH}$.

expected and **observed** limits on HH production in:

- early LHC Run 2 data (35.9 fb^{-1}),
- present using full LHC Run 2 data (138 fb^{-1})
- projections for the HL-LHC (3000 fb^{-1})

HL-LHC 3ab^{-1}: di-Higgs

CMS PAS FTR-21-004

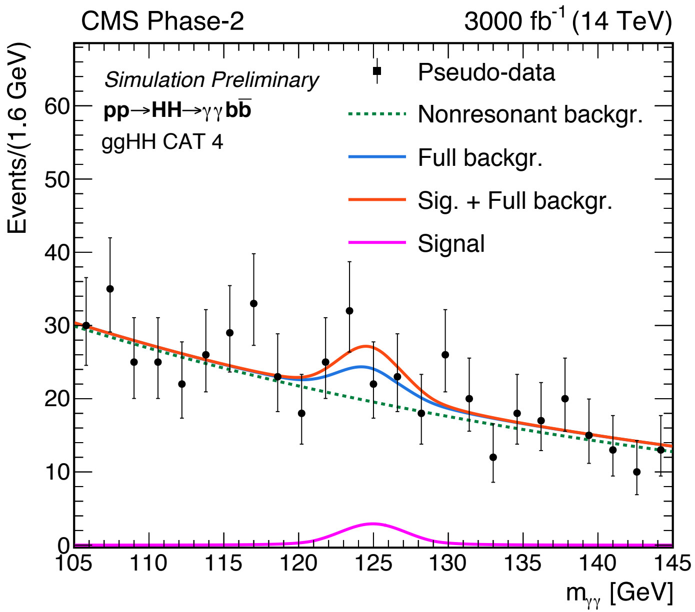

2.16σ expected sensitivity from bbγγ

Trilinear Coupling k_λ

ATL-PHYS-PUB-2022-005

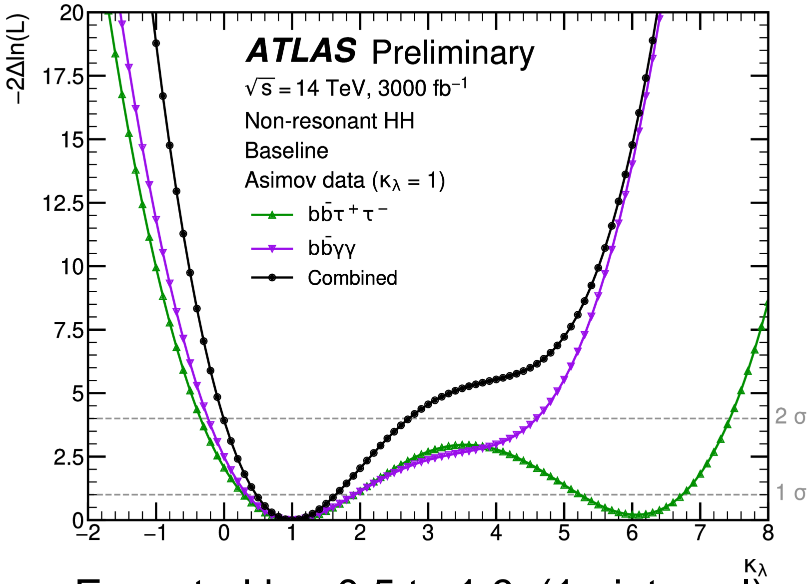

Expected k_λ : 0.5 to 1.6, (1σ interval)

bbττ+bbγγ combination: 3.2σ expected

CERN Yellow Report CERN-2019-007

ATLAS+CMS combined: 4σ sensitivity (with older projections)

With latest projections, a 5σ combined sensitivity is expected.

4-June-2024

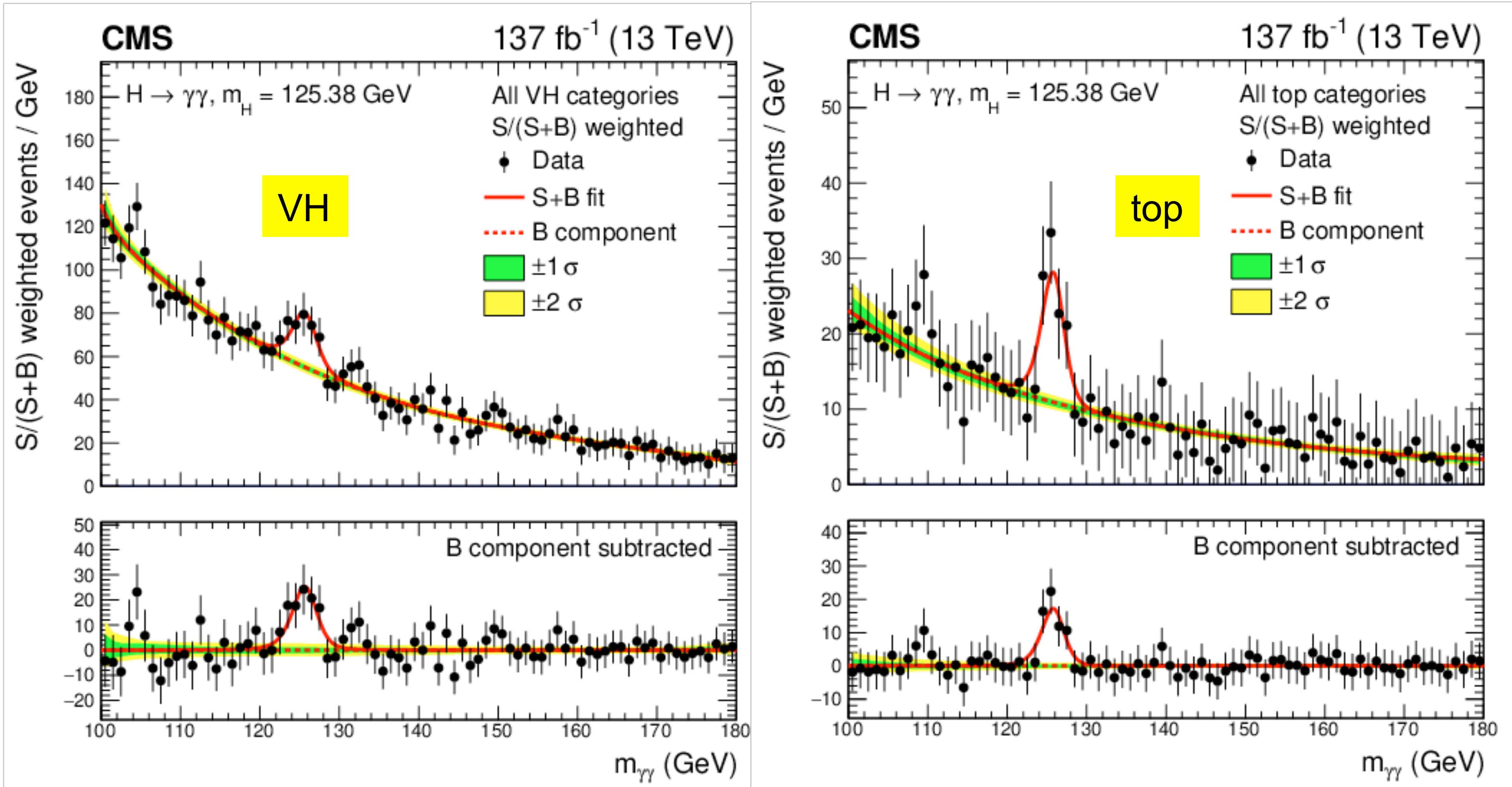
CMS
137 fb-1 (13 TeV)
H → γγ, mH = 125.38 GeV
All VH categories
S/(S+B) weighted
Data
S+B fit
B component
±1 σ
±2 σ
VH
S/(S+B) weighted events / GeV
B component subtracted
mγγ (GeV)
CMS
137 fb-1 (13 TeV)
H → γγ, mH = 125.38 GeV
All top categories
S/(S+B) weighted
Data
S+B fit
B component
±1 σ
±2 σ
top
S/(S+B) weighted events / GeV
B component subtracted
mγγ (GeV)

HL-LHC 3ab^{-1}: examples

CMS-PAS-FTR-21-001

Vector Boson Scattering

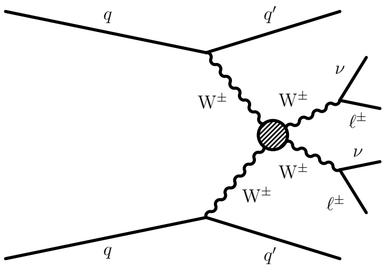

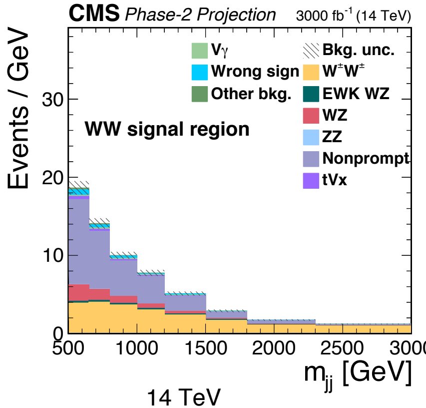

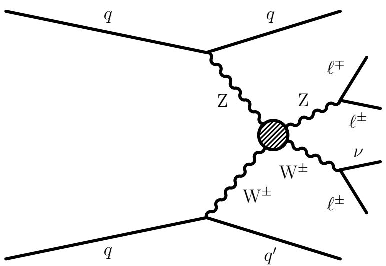

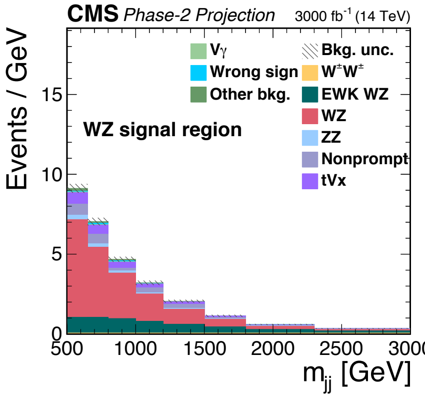

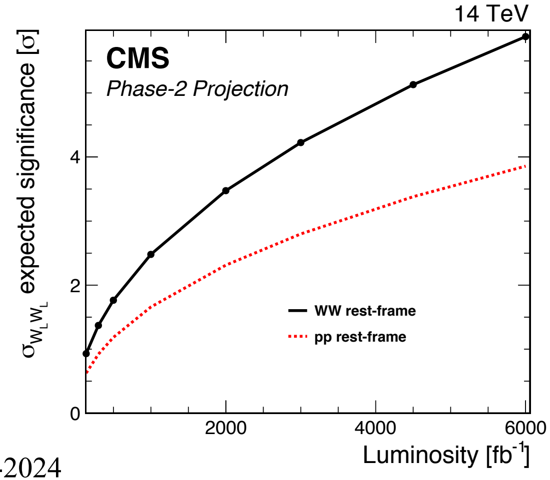

Particle Searches

- Z' (W') to leptons reach out to 6TeV (7.5TeV)
- KK excitations to ttbar to 5.7TeV
- Susy particle searches.
- LLPs
  - disappearing tracks
- Dark photons
- Dark Matter
  - mono-Z bosons

arXiv:2404.09159v1

Heavy Particle Towers and Nonlocal QFT

Stathes Paganis*
Department of Physics, National Taiwan University,
No 1, Sec 4, Roosevelt Road, Taipei 10617, Taiwan,
Leung Center for Cosmology and Particle Astrophysics,
National Taiwan University, Taipei 10617, Taiwan
(Dated: April 16, 2024)

A number of gravitation-motivated theories, as well as theories with new coloured fermions predict heavy particle towers with spectral densities $\rho(m^2)$ growing faster than e^m, a characteristic of nonlocalizable theories. It is shown that if a light scalar, like the Higgs boson, interacts strongly with a heavy scalar particle tower with exponentially rising degeneracy, then the local low-energy theory is equivalent to an effective nonlocal scalar QFT. For energies approaching the nonlocality scale $p^2 \simeq \Lambda_{NL}^2$, the scalar propagator and scattering amplitudes are modified by nonlocal factors of the form e^{p^2/Λ_{NL}^2}. The double-Higgs production measurement at the LHC is proposed as a highly sensitive probe of nonlocality at the electroweak scale.

2024

Higgs & diphoton BSM at NTU

Name	Topic/Tasks	Position
You-Ying	• SM VH→$\gamma\gamma$ and diphoton in general	Postdoc
Fasya Kuzhaimah	• Search for diphoton resonances mH < 1TeV, run 2 • Search for diphoton resonance in run 3 (later/parallel?)	PhD student (1st year)
Hong-Yi	• Search for diphoton resonances, run 3 • if possible, SM VH->$\gamma\gamma$, run 3	MSc student
Hsin-Yeh	• High mass diphoton search, run 2 (paper)	Postdoc
Dimitry Chen	• High Pt Higgs to $\gamma\gamma$, from the Z'/W'->VH mode, run 3	MSc student
Xing-Fu	• Anomalous TGC with VH->$\gamma\gamma$, run 2	PhD (finishing)